Passive acoustic monitoring of ambient noise in the Atlantic sector of the Southern Ocean

Bachelor Thesis

Sebastian Menze

Hochschule Bremerhaven

[Original photo: John Weller]

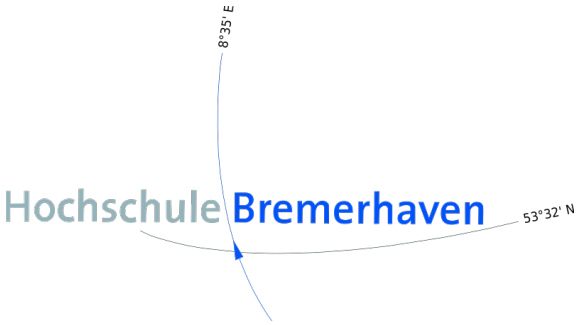

UNIVERSITY OF APPLIED SCIENCE BREMERHAVEN

BACHELOR THESIS IN THE COURSE MARINE TECHNOLOGY

Passive acoustic monitoring of ambient noise in the Atlantic sector of the Southern Ocean

12. OCTOBER 2012

Author:
Sebastian Menze
Matriculation Number:
27618

University Supervisor:
Prof. Dr. Oliver Zielinski
External Supervisor:
Dr. Olaf Boebel

"We need another and perhaps more wiser concept of animals.(...) In a world older and more complete than ours they move finished and complete, gifted with extensions of senses we have lost or never attained, living by voices we shall never hear. They are not brethren, they are not underlings; they are other nations, caught with ourselves in the net of life and time, fellow prisoners of the splendour and travail of the earth"

Henry Beston, *The outermost house* 1928

Contents

1. Abstract / Zusammenfassung

English:

Natural ambient noise in the ocean is generated by the interaction of wind, waves, ice and biological sound sources. This thesis investigates ambient noise and its dynamics at selected locations in the Atlantic sector of the Southern Ocean. The Southern Ocean provides an important habitat for marine mammals. Rising noise levels might negatively affect marine mammals, which rely on their acoustic senses for foraging, orientation and communication. Two autonomous underwater recorders were deployed on moorings at 66°S and 69°S along the zero meridian, they provided a quasi 3-year acoustic dataset which was analysed using Matlab™. A set of good environmental status descriptors, as proposed under the European Union marine strategy framework directive, was used to evaluate low frequency continuous noise. The recorded ambient noise, varying strongly over time and frequency, was correlated to ice coverage, wind speed and solar radiation. Seasonal sound pressure level change of 4.25 dB re 1 μPa was caused by the annual change in sea ice coverage. On a Weekly to sub-diurnal scale, sound pressure level variation is caused mainly by changes in wind speed. Marine mammal choruses influence distinct parts of the noise spectrum. The low frequency chorus generated by blue whales is the loudest frequency band in the ambient noise. During Antarctic winter, signals of unknown origin dominate the mid frequency part of the spectrum. The chorus of this signals exhibits a circadian rhythm at the beginning of winter. Over the 3-year recording period, a low frequency noise increase of 0.36 db re 1 μPa^2 s^{-1} at 40 hz per was detected. These findings can be used as baseline for future passive acoustic monitoring in the Southern Ocean.

Keywords:

Southern Ocean, ambient noise, passive acoustic monitoring, marine mammal chorus, good environmental status descriptors

Deutsch:

Umgebungslärm im Ozean wird durch die Interaktion von Wind, Wellen, Meereis und biologischen Schallquellen erzeugt. In dieser Arbeit wird der Umgebungslärm und seine Dynamik an ausgewählten Orten im Atlantischen Sektor des Südpolarmeeres untersucht. Das Südpolarmeer ist ein wichtiges Habitat für marine Säugetiere. Steigender Umgebungslärm kann marine Säugetiere, die auf ihre akustischen Sinne angewiesen sind um zu jagen, sich zu orientieren und zu kommunizieren, negativ beeinflussen. Zwei autonome Unterwasserrekorder wurden auf 66°S und 69°S entlang des Nullmeridians verankert. Der aufgezeichnete akustische Datensatz wurde mit Matlab™ analysiert. Dabei wurden Umweltdeskriptoren aus der "Meeres Rahmenrichtlinien Direktive der Europäischen Union" verwendet um tieffrequenten Lärm zu untersuchen. Der über Zeit und Frequenz stark variierende Lärm wurde mit der Eisbedeckung, Windgeschwindigkeit und Sonneneinstrahlung korreliert. Saisonale Schallpegelveränderung um 4.25 dB re 1 μPa wird durch jährliche Variation der Meereisbedeckung verursacht. Stündliche bis wöchentliche Variation des Schallpegels entsteht durch Änderungen in der Windgeschwindigkeit. Chöre mariner Säugetiere beeinflussen auffällige Frequenzbänder des Umgebungslärmspektrums, der Blauwal Chor ist das lauteste Frequenzband im Umgebungslärm. Während des Antarktischen Winters dominiert ein nicht identifiziertes Geräusch im mittleren Frequenzbereich das Spektrum. Der Chorus dieses Signals weist am Anfang der Winterperiode einen zirkadianen Rhythmus auf. Während der 3 aufgenommenen Jahre konnte ein Schallpegelanstieg von 0.36 db re 1 μPa^2 s^{-1} pro Jahr im 40 Hz Band gemessen werden. Die Ergebnisse dieser Arbeit können als Basiswerte für zukünftiges Passives akustisches Monitoring im Südpolarmeer dienen.

Stichworte:

Südpolarmeer, Umgebungslärm, Passives akustisches Monitoring, Chor mariner Säugetiere, Umweltdeskriptoren

2. Introduction

One of the most pristine, most remote and unexplored ecosystems on this planet is the Southern Ocean. It surrounds the frozen continent Antarctica and hold the largest current system known to men: The Antarctic circumpolar current. The intense primary production supplies a rich flora and fauna, including local and migratory populations of cetaceans and pinnipeds (see Figure 1 for Antarctic minke whale). In fact, more than 50 % of the world's marine mammals are thought to live in the Southern Ocean (Perrin et al., 2009). Because the region is highly ice covered half of the year and 400000 km away from the world's population centres, it stayed relatively untouched compared to the oceans of the Northern Hemisphere. With the rise of industrialised whaling, the Southern Ocean's cetacean populations became depleted to near extinction. Since the international moratorium on commercial whaling in 1982, the populations are expected to recover. In 1961 the Antarctic treaty entered into force. It dedicates the region South of 60°S to peaceful usage and science. In addition to the treaty, a set of environmental protection agreements exist. Climate change and industrialisation affect the whole planet, the Southern Ocean also increasingly underlies human impact.

Figure 1: Antarctic minke whale (*Balaenoptera bonaerensis*) surfacing between young sea ice. Photo from bridge camera of RV Polarstern

One of the stressors humans introduce to the ecosystem is underwater acoustic noise. Sounds, from impulsive airgun shots to the continuous noise created by ships, can alter animal behaviour and survival (Weilgart, 2007, Tyack, 2008, Blickley and Patricelli, 2010). Anthropogenic noise can have negative effects on individual animals but also on entire populations (Clark and Gagnon, 2006). Given the fact that cetaceans and pinnipeds use sound in highly specialized ways to orientate, forage or communicate, a comprehensive protection should include the regulation and monitoring of the acoustic environment. As

marine traffic and industrial activities primarily focus on the Northern Hemisphere and only slowly increase in the South, little research has been conducted on ambient noise in Antarctic waters (SCAR, 2012). This thesis aims to describe the ambient noise prevailing at selected sites in the Atlantic sector of the Southern Ocean. The following questions will be investigated:

- What does the Southern Ocean's ambient noise sound like?
- Can we define an acoustic baseline for future monitoring of ambient noise?
- What are the typical biotic and abiotic sound sources and their characteristics?
- What is the natural variability?
- Are there anthropogenic noise sources audible?
- What recommendations can be made for noise regulation?

3. Fundamentals

3.1. Hydroacoustics

3.1.1. Acoustic waves

The propagation of sound requires an elastic medium. Water is rather elastic and thus makes an excellent sound transmitter. Sound is a pressure wave, also called a longitudinal or compression wave. The energy of a wave travels through a medium trough a series of compressions and dilations. The one dimensional solution of the wave equation can be expressed by formula 1 (Medwin and Clay, 1998).

$$p = f_1\left(t - \frac{x}{c}\right) + f_2\left(t + \frac{x}{c}\right) \tag{1}$$

In this equation the functions f_1 and f_2 represent the wave travelling in the forward and backward direction, p is the pressure, t the time, x the distance and c the sound speed. Its general solution is (Medwin and Clay, 1998):

$$p = A\left(e^{j\omega(t-x/c)}\right) + B\left(e^{j\omega(t+x/c)}\right) \tag{2}$$

If we choose the case of spherical spreading of the sound wave we can calculate the pressure over time using equation 3 (Medwin and Clay, 1998):

$$p(t) = \frac{p_{re\,1m}}{R}\left(2\pi f\left(t - \frac{R}{c}\right)\right) \tag{3}$$

This equation only roughly describes the pressure a receiver will experience at any point away from a sound source. It requires an ideal point sources and a uniform propagation medium. In the real world sound sources create a complex sound field. Generally one can differentiate between the acoustic near field and the acoustic far field. The near field is characterized through zones of constructive and destructive interference, which results in areas of high and low sound pressure levels. The sound pressure in the far field decreases monotonously.

3.1.2. Sound propagation

The sound velocity is a very important variable for underwater sound. It not only determines how fast a sound travels through a medium but its variation in the water column is responsible for a variety of phenomena. The elasticity and density of a medium determine its sound speed. For sea water this means the sound speed is influenced by the quantities temperature, depth and salinity (Medwin, 2005). As a mean value, the rounded sound velocity of $1500\frac{m}{s}$ is used. But under real condition it varies in depth: At the location studied in this thesis, within a range of $60\frac{m}{s}$ over depth. It is very important to know the variation of sound speed with depth, also called the sound speed profile, because it greatly affects the propagation of sound waves in the ocean.

The recorders used in this thesis were placed around 200 m below the surface, the sound speed and temperature profiles at the recorders locations are displayed in Figure 2. The two temperature profiles show a strong positive temperature gradient between the cold surface water with -1.5° C and the warmer intermediate and deep water layers with

0.5° C. This gradient is located between 50 to 300 m depth and is frequently observed in polar oceans. Because increasing temperatures result in increasing sound speed, a strong positive sound speed gradient exists between 20 to 250 m depth. Below the thermocline, in the isothermal deep layer, sound speed increases with depth as a result of pressure increase.

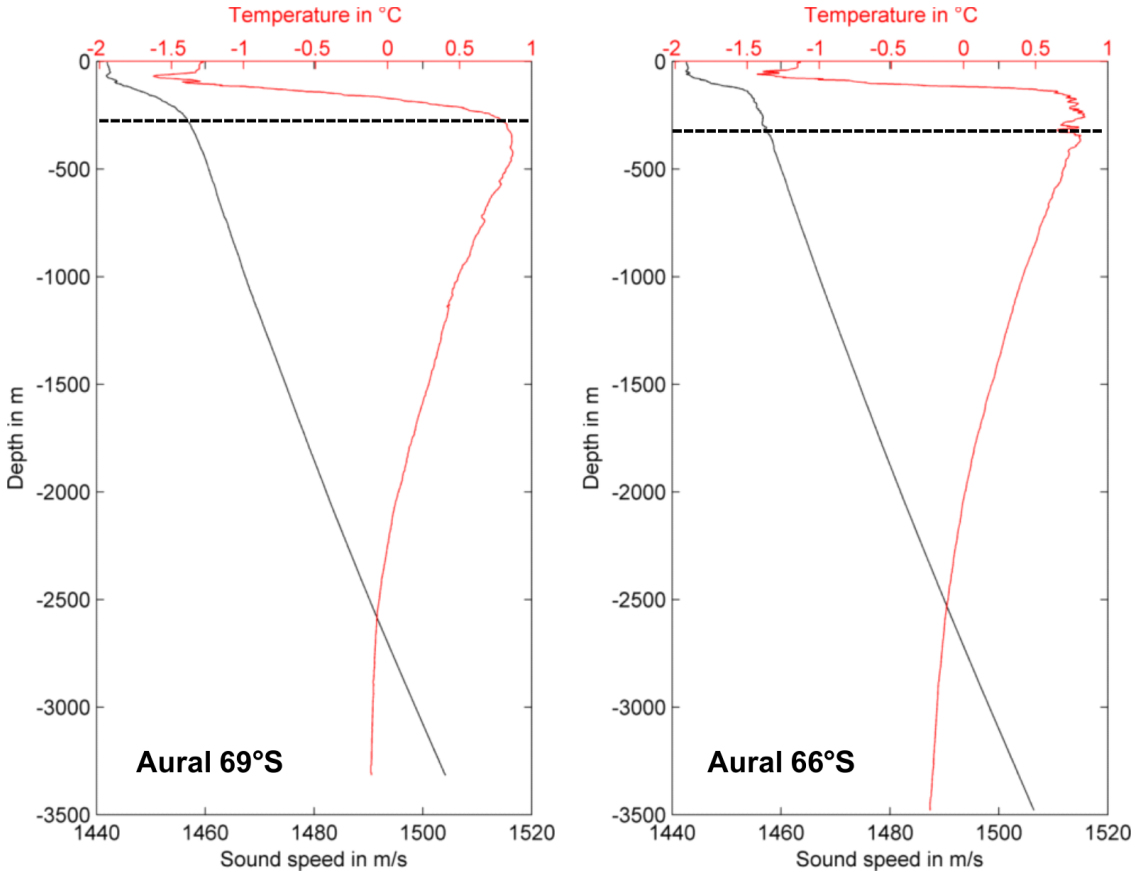

Figure 2: The two left plots show the sound speed and temperature profile at the locations of the two recorders used in this thesis. The black line represents the sound speed over depth, the red line the temperature over depth. The broken lines shows the depth in which each underwater recorder was moored. The profiles were measured using a SBE911plus and seabird CTD sensor in December 2010.

In tropical to boreal latitudes, the temperature gradient over depth in the surface layers is negative. This is a result of warm water in the surface layers, which is heated by solar radiation. With increasing depth, temperature and sound speed decrease in the thermocline. A sound channel forms between the negative sound speed gradient of the thermocline and the positive sound speed gradient of the isothermal deep layer (Medwin and Clay, 1998). It is centred around the sound speed minimum. The positions of the sound speed minimum depends on the stratification of temperature and salinity in the upper layers of the water column.

Under tropical to boreal conditions the minimum is located under the thermocline. Declining temperatures in the thermocline results in declining sound speed, until the point of minimal sound speed is reached. Below this point the increasing pressure is responsible for a gradual increase of the sound speed. If we now consider Snell's law of refraction, a sound wave entering the zone of minimal sound speed will eventually get refracted on the upper and lower boundary of the sound channel.

In the polar regions the sound speed minimum lies close to, or at the sea surface. Due to the cold surface water a positive sound speed gradient exists in the thermocline. This results in sound waves being bent upwards throughout the whole water column. This is displayed in Figure 3. At the surface the waves either get reflected by open water surface or the ice cover. The open ocean surface is an effective reflector of sound waves, but sea ice tends to absorbs sound. The rough and fractal underside of the floes scatters sound waves and acts like a low pass filter, absorbing especially high frequencies (Uscinski and Wadhams, 1999). .

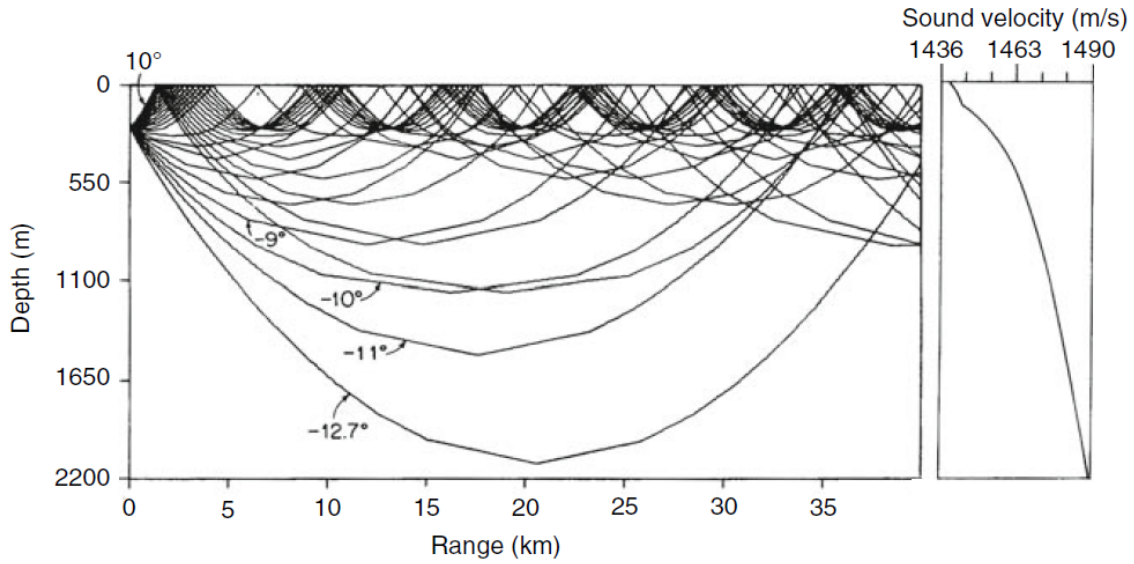

Figure 3: Raytracing diagram for a polar sound speed profile, from Urick (1983). The bending of sound waves to the surface is visible. The right side shows a typical sound speed profile for polar regions

A sound wave propagating though the ocean gets reflected at the sea surface and floor. This reflections and the refraction of sound waves in a sound channel result in multiple path propagation. A receiver will eventually record the same signal propagating along different paths. Depending on the entrance angle of the sound wave and sound speed profile, zones of constructive and destructive interference can develop. Multipath propagation can be used to calculate travel times of signals along different paths. But it can also become a problem because a signals time characteristics can be altered and "blurred". Figure 4 shows the spectrogram of a sperm whale echolocation click and its echo. Sperm whale clicks consist of two single clicks: the first is the click produced by a snapping membrane and the second is the click's reflection on the skull of the sperm whale. The time difference between the first click pair and its reflection is roughly 0.7 s.

If we assume the whale and the recorder at a depth of 200 m, the distance of the whale at the time of the first click pair was 561 m, and at the time of the second click pair 425 m. The distance is 138 m, which would results in a swimming speed of 80 $\frac{m}{s}$, a very unrealistic value. So either two sperm whales were present or our assumptions were wrong.

Sound waves emitted by a point source in an infinite ideal medium will spread spherical. This implies a so called geometric transmission loss. Considering the conservation of energy, the pressure per unit area decreases with the square of the distance to the point source (Lurton, 2002). Additional to spherical spreading loss, cylindrical spreading loss occurs. When assuming cylindrical spreading loss, the sea surface and floor act as boundaries, so sound waves can only propagate in two dimensions. In this case the pressure per unit area decreases linear with the distance to the source. This is only a rough estimate under ideal conditions, but helps to understand the characteristics of sound waves in the ocean. To exactly determine the sound field and wave propagation, advanced models and acoustic ray tracing programs have been developed.

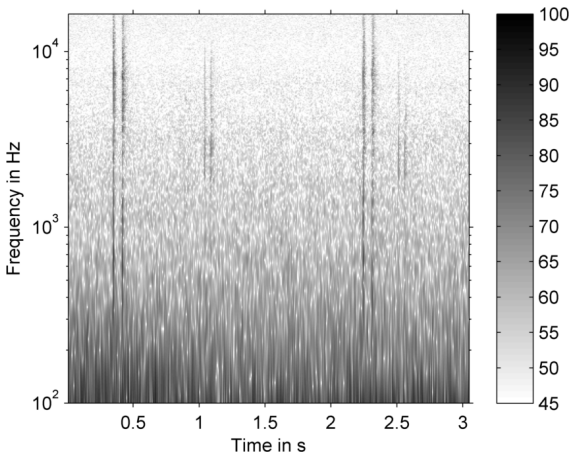

Figure 4: The spectrogram of a sperm whale echolocation click, recorded with Aural-M2 autonomous recorder at 0.07°E and 66°S. The direct and the reflected click pairs are visible. The Colour bar shows the PSD in db re 1 μPa^2 s^{-1}

The transmission loss of an acoustic signal is a combination of geometrical spreading loss and dissipation of the energy into thermal energy. In sea water the absorption is caused by the effects of viscosity, ionic relaxation of magnesium sulphate molecules and a boric acid ionization process (Medwin and Clay, 1998). High frequencies get absorbed faster than low frequencies.

3.1.3. Sound measurement and processing

To record and measure sound in air, microphones are used. In liquids hydrophones are used. Just like their counterpart in air they consist of a transducer that converts the pressure oscillations into voltage oscillations. The transducers used in hydrophones are often made from piezoelectric crystals such as the ceramic materials barium titanate or lead zirconate titanate (PZT) (Au and Hastings, 2008). The signal oscillations excited by the transducer gets pre-amplified depending on hydrophone type and purpose. The voltage then gets band pass filtered to avoid aliasing and sampled by an A/D converter. The now time and amplitude discrete signal is stored on a hard drive or another digital memory.

When dealing with analogue or digital signals one decides between two domains: The frequency and the time domain. In the time domain the amplitude (in our case pressure) is observed over time, this is usually called the waveform of a signal. In the frequency domain the amplitude of the signal is plotted over frequency, this is called the spectrum. A combination of these two methods is the spectrogram which contains time, frequency and energy information. The x and y axis represent time and frequency, the z axis, usually displayed as colour, represents the amplitude. In this way a compact but informative graphical representation of a signal is created.

To measure the pressure of a sound wave the current from the hydrophone is calculated to μPa. In acoustics, the amplitude of pressure waves is defined sound pressure level (SPL). Because the pressure oscillations in a sound field vary at great magnitudes, the SPL scale was defined as logarithmic scale to the base of 10. The definition gives the SPL in decibels (Medwin, 2005):

$$SPL = 20 \cdot log_{10}\left(\frac{p}{p_{ref}}\right) \tag{4}$$

To define a scale, a reference value is necessary. In the case of hydroacoustics the reference pressure is $1\mu Pa$. In air the reference pressure is a different one: $20\mu Pa$ (human hearing threshold). This fact makes it difficult to compare the SPL in air and water. Because of the different reference levels, one has to subtract:

$$20 \cdot log_{10}\left(\frac{20\ \mu Pa}{1\ \mu Pa}\right) = 26.02\ dB\ (air - water\ reference\ level\ difference) \tag{5}$$

to compare in-water SPL to in-air SPL on the decibel scale. Also the impedance of water and air greatly differs. The comparison of intensities is described by equation:

$$\frac{I_{air}}{I_{water}} = \frac{\left(\frac{p^2}{\rho c}\right)_{air}}{\left(\frac{p^2}{\rho c}\right)_{water}} \tag{6}$$

Assuming that sound speed in water is 1500 m/s and the density of water 1.026 kg/m3 and for air the sound speed reads 344 m/s at the density 1.21 kg/m3 (Lurton, 2002), the ratio of pressure is:

$$\frac{p_{water}}{p_{air}} = \sqrt{\frac{(\rho c)_{water}}{(\rho c)_{air}}} = 60 \tag{7}$$

The combined sound intensity level difference between air and water on the decibel scale is:

$$26.02\ dB\ +\ 20 \cdot log_{10}(60)\ =\ 62.16\ dB\ (air - water\ difference) \tag{8}$$

Sound pressure levels of equal intensity are 62.16 dB higher in water than in air. The different reference levels and the dB scale have caused some confusion in media and public discussion. Now we know the SPL of every sample in the recording, but what is needed is an averaged value. In this thesis I used the root mean square (RMS) method. Every sample gets squared, then a mean value is calculated and its square root is the RMS value.

$$SPL_{RMS} = \sqrt{\frac{1}{n} \cdot \left({p_1}^2 + {p_2}^2 + ...{p_n}^2\right)} \tag{9}$$

Using the RMS method is not uncritically because, for non stationary signals, the SPL_{RMS} changes with the number of averaged samples n . This is especially the case when impulsive sound sources are present. In this case one should also determine the peak-to-peak values of a signal (Madsen, 2005). Also the averaging method for SPL values has been discussed, Merchant et al. (2012) recommend to use the mean instead of the median to average SPL values. For the purpose of examining continuous ambient background noise, root mean square averages are suitable.

To represent a signal in frequency space one has to calculate its Fourier transform. The Fourier theorem basically states that every signal can be replaced by an infinite number of sine and cosine signals. For discrete operations it is described by equation 10 (Smith, 2003):

$$x[i] \;=\; \sum_{k=0}^{N/2} \overline{X}_{real}[k]\; cos\left(\frac{2\pi ki}{N}\right) + \overline{X}_{imaginary}[k]\; sin\left(\frac{2\pi ki}{N}\right) \tag{10}$$

It describes the synthesis of the Fourier transform from a digital signal of the size N: $x[i]$ is the signal being synthesised (i runs from 0 to N-1) and $\overline{X}_{real}[k]$ and $\overline{X}_{imaginary}[k]$ hold the amplitudes of the sine and cosine waves that represent the signal, with k running from 0 to $N/2$. There are different algorithms to compute the Fourier transform, the most used is the Fast Fourier Transform (FFT). It needs little computation time and is implemented in most signal processing systems. The synthesised sine and cosine signals can now be averaged and weighed over time using different methods. In this thesis, Welch's method was used to calculate the power spectral density (PSD) of the acoustic signals. The power spectral density gives information about the distribution of power over frequency in $dB\ re\ 1\ \frac{\mu Pa^2}{Hz}$.

In acoustics the concept of octaves is often used. An octave describes the frequency ratio between a frequency f and $2 \cdot f$. To achieve a higher frequency resolution this space can be divided further, often third-octave bands are used. The centre frequencies of the octave bands are usually aligned around 1 kHz. Since it is widely implemented in technology and standardisation, octave bands are used to analyse and regulate sounds.

3.2. Ambient Noise

In this thesis, sounds are classified into two categories: Continuous and transient sounds. Transient sounds occur only for a short period of time (milliseconds to minutes) and are not considered to be a part of the ambient noise described in this thesis. Continuous sounds or noise form a part of the background noise and last as long as hours or month. In this thesis, ambient noise is defined as the continuous background noise present on the scale of hours to years. Transient sounds are not investigated in this paper.

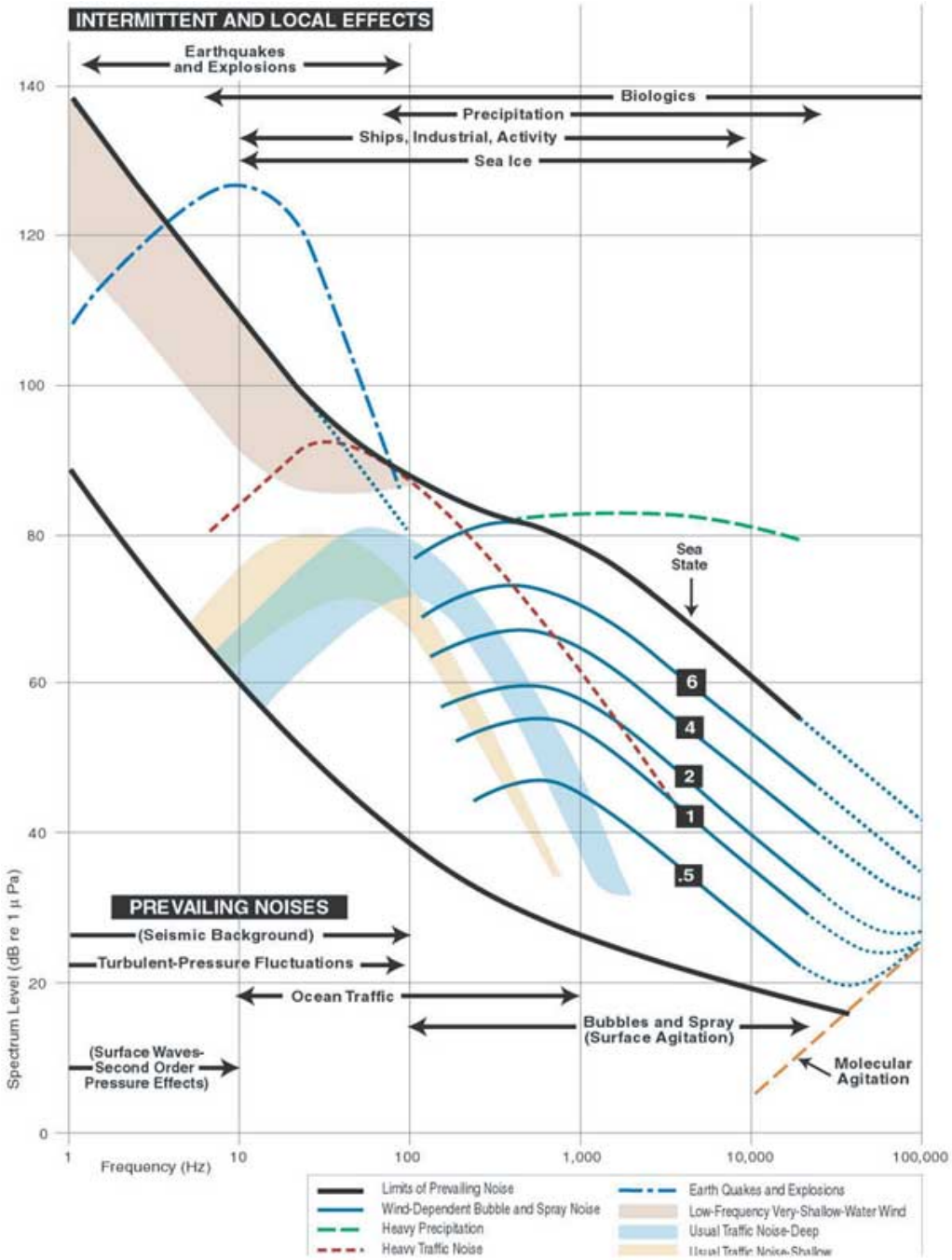

Figure 5: A composite of ambient noise spectra, compiled by Committee on Potential Impacts of Ambient Noise in the Ocean on Marine Mammals (2003) after Wenz (1962)

3.2.1. Sources

As stated before, sea water is an excellent transmitter of sound. The absorption of sound waves in water is minimal compared to air. This condition results in high noise levels. Ambient noise is generated by multiple sources. This can be: Wind, waves, earthquakes,

ice motions, thermal noise, biological and anthropogenic sources. The much cited paper "Acoustic Ambient Noise in the Ocean: Spectra and Sources" by Wenz (1962) reviews and describes the dependence of ocean ambient noise on several environmental parameters. Figure 5 shows the summary of his investigation and gives information about the dominant noise spectra in the worlds oceans.

Wind and Waves:

The agitation of the sea surface is the main generator of broadband noise. The sound of breaking waves, familiar to us from beaches, is one type of wind induced noise. Surface waves generate noise trough several mechanisms: At first, there is the breaking of the wave itself followed by the induction of air bubbles into the water column (Medwin and Clay, 1998, Ma et al., 2005). These bubbles oscillate and eventually collapse. Then there is flow noise itself, generated by the wind dragging over the sea or ice surface. The exact processes and their contributions to the noise spectrum are not fully understood yet. According to the model by Wenz (1962), wind generated noise approximately dominates the spectrum from 100 hz to 50 kHz and wave and bubble cloud generated turbulences the spectrum from 20 to 500 Hz. Nichols (1981) reported a strong correlation of wind speed with noise in the 0.1 to 10 Hz band. The dependence of noise and wind speed was described by Knudsen et al. (1948), they developed a model for wind speed dependent noise in the 1 to 100 kHz Band. This model is used widely to estimate the noise levels in the frequency range of sonars, as it focuses on high frequencies.

Precipitation:

When falling rain or hail hits the sea surface it generates noise trough the impact itself and oscillating and collapsing bubbles under the surface. Depending on the intensity and drops size rain noise varies in sound pressure level and spectrum. The general assumption is that rain noise covers frequencies from 1 to 50 kHz and drop size correlates well with source level. Ma et al. (2005) conducted research to measure rain drop size distribution with acoustical rain gauges and successfully monitored the weather above the surfaced with submerged hydrophones. With the use of adapted algorithms and reliable technology it is possible to conduct rain and wind speed measurements using passive acoustic monitoring (Medwin and Clay, 1998).

Earthquakes and other infrasounds:

In the deep frequent areas of the ambient noise spectrum, also called the infrasonic region it is difficult to distinguish acoustic and seismic waves. The border between low frequency acoustic sources in the ocean (wave and tide related) and seismic sound sources (earthquakes and microseisms) blurs, as pressure waves generated in the earth crust travel trough the ocean and waves of oceanic origin enter the crust (Medwin and Clay, 1998). Infrasonic sounds cover frequencies below 20 Hz and are not audible to the human ear. The average hearing threshold for humans is 20 Hz to 20 kHz in air. Earthquakes are not part of the continuous background noise as they occur only spontaneous, but microseisms and other deep frequency waves contain the most energy of the ambient noise spectrum. This happens due to the extreme source levels and little absorption they

do experience. The exact processes that govern infrasonic sounds in the ocean are not fully understood yet. Additionally to the physical sources, several baleen whale species produce infrasound (Au and Hastings, 2008). This will be discussed in detail in the section dealing with biological sound sources. The loudest sound detected in the recordings analysed in this thesis was an earthquake.

Thermal:

On the other side of the acoustic spectra we deal with very high frequencies. Thermal agitation of the surrounding water molecules and in the electronic circuits will generate noise, increasing with frequency (Lurton, 2002). This effect can be ignored for frequencies up 50 kHz, but increasingly dominates the spectrum and becomes the main source of noise above 500 kHz. As recordings in this thesis only cover a frequency range from 10 hz to about 16 kHz, the effects of thermal noise can be ignored.

Ice:

Compared to mid and low latitude seas, the polar oceans form a unique acoustic environment. They are seasonally ice covered and feature an upward refracting sound channel. The sound speed minimum lies at or very close to the surface, due to the influence of the cold surface water on the sound speed gradient. Sea ice and icebergs produce a broad variety of sounds, from the extremely loud screaming and break-down sounds of colliding icebergs to the quiet cracking of melting ice (Pritchard, 1990, Milne, 1972, Kibblewhite and Jones, 1976). Although most ice generated sounds are transient, they can influence the ambient noise (Uscinski and Wadhams, 1999). Typical sounds include cracks, roars, singing and screaming noises, as well as hissing sound. These sounds are generated by the collision, deformation, ridging, rafting and shearing of ice floes or ice bergs.

The ice cover does not only generates sounds itself, but passively affects the prevailing ambient noise. It reduces the surface agitation and dampens the effects of wind and waves on the ambient noise spectrum. Ambient noise during ice covered and open water periods differs greatly in SPL and spectral composition.

Biological:

Next to the previously described physical sources, marine fauna partly contributes to ambient noise. Many marine animals have adapted the use of sound for different purposes, such as communication, orientation and foraging. Especially cetaceans are well known for their abilities to produce sound. If a vocalisation is abundant enough, it becomes part of the ambient noise and each vocalisation type forms its corresponding noise band, also referred to as chorus. These choruses, not individual vocalisations, are analysed in this thesis.

The order cetacea, consists two suborders: The odontoceti, known as toothed whales, and the mysticeti, known as baleen whales. Odontoceti have developed echolocation, which allows them to navigate and forage with the use of sonar like clicks (Au and Hast-

ings, 2008). They are also known to produce social sounds like whistles and grunts. As most animals of the suborder developed vocalisations consisting of high frequency and impulsive sounds, the odontoceti contribute little to ambient noise. But transient vocalisations from killer whales (Orcinus orca), Sperm whales and others odontocetis can be heard frequently in the Southern Ocean. Unlike the toothed whales, baleen whales do not posses a high frequent biosonar and their vocalisations are usually in the mid to low frequency region (Au and Hastings, 2008). As low frequency calls get absorbed less and mysticeti vocalisations are very abundant in the Southern Ocean, certain frequency bands in the spectrum are influenced by mysticeti vocalisations.

Anthropogenic:

Noise generated by human activity plays an increasingly important role in the global noise budget. The main sources of anthropogenic noise are industrial activities, seismic exploration, sonars and shipping noise (Hildebrand, 2009). Of these especially the shipping noise is thought to contributes to globally rising ambient noise levels (McDonald et al., 2006). The loud and low frequency pulses of airguns, used for seismic surveys, can be heard frequently in the North Atlantic (Nieukirk et al., 2012) and the Arctic (Moore et al., 2011). Container and other commercial vessels are equipped with heavy machinery that produces a loud noise. Machinery sounds radiate trough the ships hull and the ships propellers produce cavitation and flow noise. A modern container vessel produces noise source levels from $179 - 192$ *db re* 1 μ*Pa at* 1 *m* measured in the keelward direction (Arveson and Vendittis, 2000). Ship radiated noise is not uniform and varies with vessel speed and working mode Mckenna et al. (2012). The noise is not distributed uniformly around the ship but shows directionality depending on ship type and observed frequency. Noise levels due to cavitation and propeller rotation generally reach peak levels at the stern side of the ship Arveson and Vendittis (2000). Adding to this, some ships are equipped with high energy sonars that cover a broad frequency range. The ambient noise frequency band attributed to shipping reaches from 20 to 500 hz. Measurements by Wenz (1962) indicate that this accounts for large proportions of the oceans.

3.2.2. Development

During the last 50 years the number of sea going merchant vessels more than tripled (Hildebrand, 2009). Also the gross tonnage and size of the vessels increased. The number and size of ships is linked to global economic growth and the ongoing industrialisation. This increase in ships lead to an increase of low frequency ambient noise: McDonald et al. (2006) calculated an ambient noise increase of 3.3 dB db re 1 μPa at 40 Hz per decade. As Wenz (1962) reported, noise in this frequency region is attributed to shipping. In Figure 6, the increase in low frequency ambient noise is displayed in relation to the increase of global ship gross tonnage and global domestic product. Frisk (2012) related the rise of global gross tonnage to ambient noise increase, and thus the global domestic product to the rising noise levels. The increasing noise raised many concerns, several studies reported negative effects of anthropogenic noise on wildlife (Tyack, 2008, Blickley and Patricelli, 2010).

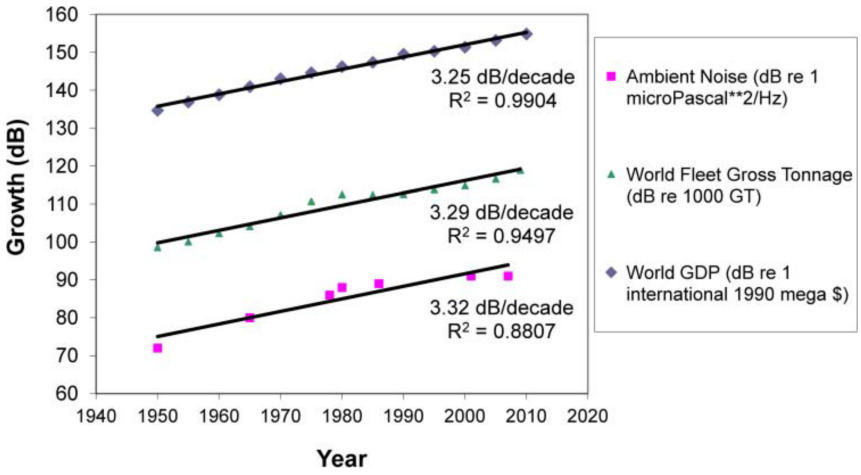

Figure 6: Plot shows increase in low frequency ambient noise, world gross tonnage(GT) and world gross domestic product (GDP) on a decibel scale, compiled by Frisk (2012)

The ships travelling across the worlds oceans are not spread uniformly but follow defined routes. These are set by economic demands as well as geographic and politic limitations. Figure 7 shows a global map of shipping intensity. It can be seen that most ship traffic is located on the Northern Hemisphere, this is a result of the current state of the world economy. A look at the Southern Ocean reveals minimal shipping intensity compared to the rest of the world oceans. This thesis aims to investigate in the ambient noise present in the Southern Ocean, and to determine a baseline for further noise monitoring.

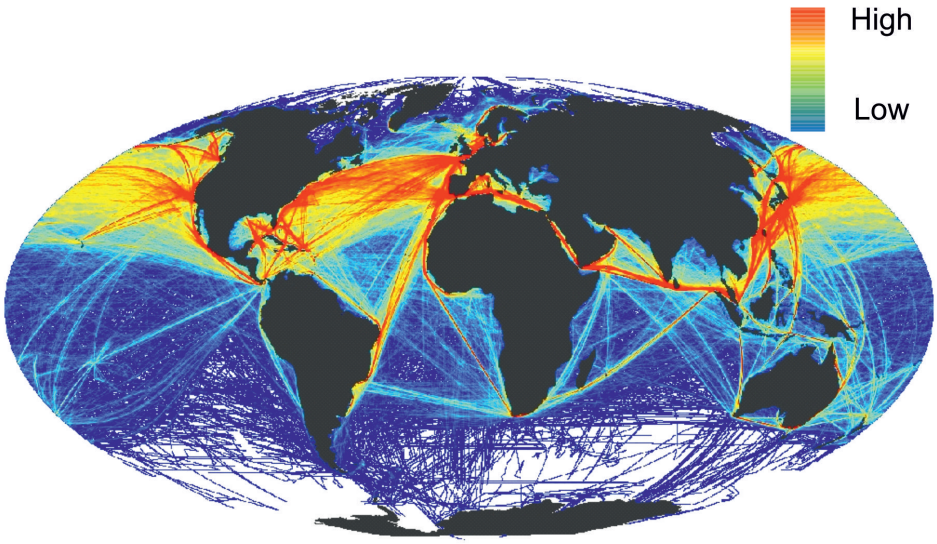

Figure 7: Global Map of shipping intensity by Halpern et al. (2008). Colors indicate shipping intensity in number of ship tracks per 1 km^2 cell, Values reach from 0 to 1158 ship tracks per 1 km^2 cell, Averaged from 2008 to 2009

3.3. Effects of noise on marine life

The increasing level of shipping noise led to discussions about possible impacts on marine life. Both transient high amplitude sounds and continuous low level noise can endanger aquatic animals. The rising awareness of this has led to various research activities and a demand for detailed studies of the oceans soundscape (Blickley and Patricelli, 2010).

3.3.1. Mechanisms

The impact of sound on animals varies with intensity and frequency. If the sound lies with in the animals hearing range, it's effects can be graduated from mere detection of the sound, masking of other relevant sounds, disturbing the animals behaviour, causing temporal threshold shift (TTS) to causing permanent threshold shift (PTS) (Weilgart, 2007, Tyack, 2008, Clark et al., 2009). In the case of continuous background noise, especially masking and disturbing effects are relevant. As shipping induced noise levels rise comparatively fast on an evolutionary scale, reliable information on the risks and possible mitigation measures have to be gathered. In the case of high energy impulse sounds, such as airguns or wind farm construction sites produce, the risk of TTS and PTS have to be evaluated (Di Iorio and Clark, 2010). Which noise is dangerous and how far these effects endanger individual animals or whole populations is still theme of scientific debate. Often the border between transient and continuous noise and their effects are hard to diminish. Also an animals behaviour in the presence of noise is difficult to predict, as some animals observed avoid the sound source, whereas others appear to be attracted by it (McCauley et al., 2000).

3.3.2. Cetaceans

The order believed to be most endangered by underwater noise is the cetaceans. They have developed highly specialised acoustic senses and rely on them for communication, orientation and foraging (Au and Hastings, 2008). Many odontoceti use biosonar to locate and track their prey as well as to communicate and locate each other. Baleen whales emit low and mid frequency calls and songs. Those can be heard over hundreds of kilometres. Sirović et al. (2007) located blue whale calls 200 km away. As the population densities of baleen whales are usually small, caused by natural migration patterns and whaling, long range communication is vital for the reproduction of a population. With the dramatic increase in traffic noise, their communication range is likely to be reduced and requires an adaptation (Ospar, 2009). Together with other risks like ship strikes, reduced habitat and pollution this executes high pressure on already endangered species (Tyack, 2008). The consequences and mechanisms of masking and disturbing cetaceans through shipping noise are not completely understood and require further investigation.

Whales directly exposed to a loud anthropogenic sound source can be in danger of TTS and PTS (Ospar, 2009). But even if not loud enough to cause a threshold shift, high amplitude sounds can harm an animal. A much studied source of harmful noise is the use of mid frequency active sonar (MFAS). These systems emit sound at extremely high source levels and cover large areas of the ocean. Several strandings of beaked whales have been related to navy manoeuvres using MFAS (Boyd, 2008). The sonar signals

appear to have altered the whales behaviour and caused them to rapidly flee, possibly causing hypothermia. In the Arctic, a study observed 250 fin whales stopping their calls over weeks while seismic air gun arrays were operating, but returning to their natural vocalisation behaviour within hours after the survey stopped (Clark and Gagnon, 2006).

3.3.3. Pinnipeds, Fish and other

Pinnipeds have ears adapted to hear both in air and water. Many species produce a variety of sound in both media, and use their vocalisations mainly to communicate (Van Opzeeland et al., 2010). Controlled exposure experiments showed that some seals suffer a threshold shift when exposed to loud sounds (Kastak et al., 2005). Most pinnipeds hear best at mid to high frequencies. Like cetaceans the negative effects noise can have on seals reach from masking of communication calls to behaviour change and even PTS.

3.4. Noise Regulation

Environmental law and international policy have yet to adapt to this relativity recent development (Scott, 2004). The stranding of beaked whales caused by military sonar in the Mediterranean sea and the Bahamas caused an uproar in the public, and the scientific evidence for the negative effects of some noise sources began to grow (Weilgart, 2007). The demand for national and international policies to protect marine wildlife against high noise levels rose and first nations passed laws.

In the EU, the Marine strategy framework directive provides a tool to implement transnational regulations into national law. A set of good environmental status indicators (GES) is used to monitor the ecosystems and launch mitigation measures if the GES deteriorates. Anthropogenic noise is part of descriptor 11: Underwater noise and other forms of energy (Commission, 2010). The descriptor gives 2 indicators. The first concerns loud low and mid frequency impulsive sounds, such as those produced by wind farm construction or airgun operation. The following GES indicators are expected to improve:

"Proportion of days and their distribution within a calendar year over areas of a determined surface, as well as their spatial distribution, in which anthropogenic sound sources exceed levels that are likely to entail significant impact on marine animals measured as Sound Exposure Level (in db re 1 $\mu Pa^2.s$ *) or as peak sound pressure level (db re* 1 μPa_{peak}*) at one metre, measured over the frequency band 10 Hz to 10 kHz"*

The second indicator requires that the trend in low frequency continuous noise should not rise in the third-octave frequency bands with the center frequencies 63 hz and 125 hz. This third-octave bands were choosen to represent shipping noise. The second indicator expects a decrease of the following trends:

"Trends in the ambient noise level within the third-octave bands 63 and 125 Hz (centre frequency) (in db re 1 μPa_{RMS}*; average noise level in these octave bands over a year) measured by observation stations and/or with the use of models if appropriate"*

4. Materials and Methods

4.1. Passive acoustic monitoring

Passive acoustic monitoring (PAM) is a simple but powerful method. The basic principle is to record naturally occurring sound in the ocean and extract relevant information from it via signal processing. This can be done with a single hydrophone on a recorder or with an array of hydrophones. The latter approach has the advantage of including directional information. For real time observations, hydrophones can be cabled to a receiving station, towed in an array behind a ship or connected to a radio transmitter. The main applications of PAM are:

- Detection, classification, localisation and quantification of vocally active animals
- General observation of soundscape
- Noise measurements
- Behavioural studies

PAM is widely used in science, but also in industry. Several industrial operations in the marine realm, such as seismic surveys, loud construction work or mine clearance require parallel PAM to detect marine mammals in the vicinity. For this thesis autonomous underwater recorders with single hydrophones were used.

4.1.1. Underwater Recorders

The acoustic data described in this thesis was recorded with two Aural-M2 (Autonomous Underwater Recorder for Acoustic Listening - Model 2) underwater recorders, manufactured by Multi-Électronique (MTE) Inc. in Canada. Figure 8 shows the recovery of an Aural-M2. They consist of a steel and fibreglass pressure housing which holds the batteries, electronic boards and a hard drive. A HTI-96-MIN hydrophone is connected to the recording unit with a Subconn underwater connector. The batteries used, were 12 V Alkaline cells with a total capacity of 240 Ah. The sampling schedule consisted of 5-min recordings every 4 hours, starting at 00:00 daily. During operation, the recordings were at first stored in the internal RAM of the circuit and were regularly saved as .wav waveform files on a hard drive. Software problems resulted in noisy files every 48 recordings. The entire noisy files were sorted out afterwards using a Matlab™ routine. The system was configured to record with a sampling frequency of 32768 Hz and 16 bit resolution. An ATA 120 GB hard drive provided enough memory to record at least 3 years. In Table 1, an overview of the recorders set-up is given , the manufacturers specifications sheet is attached as Figure 35 in Appendix C.

Table 1: Set-up of the deployed Aural-M2 recorders

Bit depth	16 bit
Sampling frequency	32.768 kHz
Dynamic range	42 to 149 dB
Frequency range	10-32768 Hz
Timebase	32768 Hz TCXO
Anti aliasing filter	8th order linear phase low pass

Figure 8: Recovery of Aural-M2 recorder from a mooring in the Fram Strait

4.1.2. Location and Fieldwork

Two AURAL-M2 recorders were deployed in oceanographic moorings along the Greenwich merdian in the Atlantic Sector of the Southern Ocean. Their locations are displayed in Figure 9. One Aural was located at 68.9957 °S and 0.0028°E at 260 m depth, the other at 66.0187°S and 0.0795°E at 218 m depth. The Aurals will further be referred to as Aural 66°S and Aural 69°S. The moorings were part of an oceanographic long term study, where every mooring gets an ID indicating position and series: Aural 66°S was in mooring AWI-230-6 and Aural 69°S in AWI-232-9. Dyneema rope was used as mooring line. The moorings consisted of multiple instruments, the detailed mooring schemes can be found in Appendix C. With a 1 t bottom weight and glass floatation of approximately 500 kg buoyancy on top, a static position of the moorings in the water column was achieved. However, due to currents the moorings were sheared from their ideal upright position. The recorders depth varied within a range of 2 m for Aural 66°S and 5 m for Aural 69°S. This had no significant impact on the recordings of Aural 66°S, but the recordings of Aural 69°S contained significant amounts of mechanical noise. Both Aurals were deployed

and recovered with RV Polarstern, on the expeditions ANT-XXIV/3 and ANT-XXVII/2, respectively. The mooring period for Aural 66°S was from the 11 March 2008 to the 19 December and for Aural 69°S from the 8 March 2008 to the 16 December 2010. This quasi 3-year record provides a sufficient picture of the annual variation of the Southern Oceans soundscape.

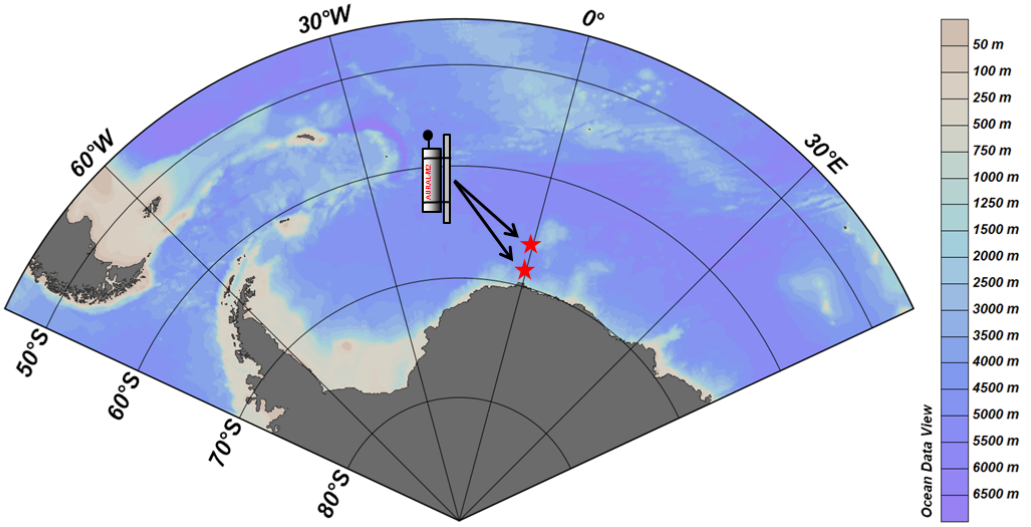

Figure 9: Location of the Aural-M2 underwater recorders, map created with Ocean data view provided by Schlitzer (2012)

4.2. Digital signal processing using Matlab™

After recovering the recorder the .wav files were transferred to a workstation computer. Here the files were at first stored and named after their origin and date using a Matlab™ routine written by Lars Kinderman. The raw dataset consisted of over 6000 5-minute long .wav files per recorder, with a total size of 110 GB per recorder.

To roughly differentiate between ambient noise and transient sounds, I wrote a script which determines the quietest 10 seconds per file (in Listing 1 of Appendix C). I choose this window length as compromise between temporal resolution (shorter window lengths increase likelihood of capturing only ambient noise) and spectral resolution (Longer window lengths result in extended frequency range and better averaging). The algorithm subtracts the cumulative sum of the squared signal, with an offset of 10-s. From this running mean (with a window length of 10-s) the minimum is determined and the 10-s snippet of the original .wav stored as variable. This selectivity filter creates a mean offset of 1.4 dB for Aural 66°S and 2.2 dB for Aural 69°S, between the 5-min and quietest 10-s window for broadband SPL_{RMS}. All further calculations and results base on this 10 s section of each file.

A flow chart of the data processing is displayed in Figure 10. I calculated the mean broadband SPL from the 10 s files. The power spectral density (PSD) of the 10-s snippet was calculated after Welch's method, using the built in Matlab™ function pwelch.m, with an FFT size of 65536. Since the samplerate is 32768 Hz, after the Nyquist–Shannon sampling theorem the highest detectable frequency is 16384 Hz. The size of one frequency bin then is $\frac{samplerate}{FFTsize}$ = 0.5 Hz.

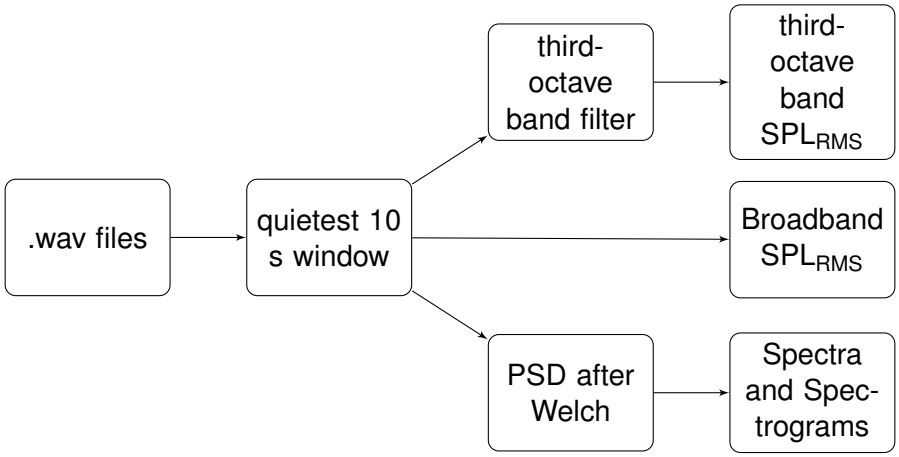

Figure 10: Flow chart of the data analysis process

To analyse noise in the two frequency bands given by the EU Marine Framework directive, I filtered the 10 s recording with a 3^{rd} order Butterworth bandpass filter. For the third-octave band filter centred at 63 Hz, the upper and lower boundaries of the bandpass filter were 56.13 Hz and 70.71 Hz. For the third-octave band filter centred at 125 hz, the bandpass filter reaches from 111.36 to 140.31 Hz. The filters were designed using the function Nth_octdsgn.m by Edward L. Zechmann, which implement the American National Standard on Specification for Octave-Band and Fractional-Octave-Band Analog and Digital Filters (Acoustical Society of America, 1986). The values for each file were stored chronologically into a structure array. Selected parts of the Matlab™ code used to analyse and visualise the recordings can be found in Appendix C.

4.3. Additional data

To investigate the dependence between ambient noise and environmental parameters the recordings were compared with wind speed, solar radiation and ice coverage. Depth data was logged by the Aurals and will be used later to explain the occurrence of system noise.

4.3.1. ECMWF meteorological model data

To investigate the relationship between wind speed and noise, I used meteorological data provided by the European Centre for Medium-Range Weather Forecasts (ECMWF). The Alfred Wegener Institute has access to data from the Operational Atmospheric Model. The variables (latitude and longitude component of wind speed at 10 m above mean sea

level, air temperature 2 m above mean sea level and mean sea level pressure) are stored on a polar stereographic grid for both poles. The cell size of the grid is 1.125° x 1.12 5°, in kilometre this is about 125 x 125 km. The time resolution of the model gives 6 h mean values. I extracted the wind speed over time from the grid cell above each Aural, with a Matlab™ script that is presented in Listing 2.

4.3.2. Ice cover and solar radiation data

The sea ice coverage data was provided as daily means by the University of Bremen and the Polar view project. It was derived from radiometer measurements with the Advanced Microwave Scanning Radiometer for EOS (AMSR-E) installed on the satellite AQUA (Spreen et al., 2008). The data is stored as daily mean values on a polar stereographic grid with a spatial resolution of 6x4 km. The values range from 0 to 100 % ice cover. Based on an indexed grid by Daniel Zitterbart, I wrote a Matlab™ routine (Listing 3) to extract the data at the Aurals positions from the grid, and store it into the structure array.

The solar radiation data was calculated from a model by the Scripps Institute of Oceanography in Matlab. It is based on the expressions given in Appendix E in the 1978 edition of the Almanac for Computers by the Nautical Almanac Office of the U.S. Naval Observatory. I calculated the daily mean solar radiation, for the locations of the Aurals, as an indicator for seasonal variability in the ambient noise.

To correlate the acoustic with the environmental data, the sample rate of both measurements need to be synchronised. For the meteorological data, this was achieved with a script that searched the values at the time of the recording, or estimated the mean of the previous and next data point, if the recording happened between two ECMWF data points . The daily means of sea ice and solar radiation data were assigned to the 6 files of each day.

5. Results

5.1. Sound pressure levels

The root mean square sound pressure level (SPL_{RMS} re 1 μPa) was calculated for the quietest 10 s per recording. This value was estimated for the unfiltered broadband recordings and the two third-octave bands centered around 63 and 125 Hz. Figure 11 displays the three SPLs for both Aurals over the 3 year recording period as well as the distribution of the SPL in histograms. Within all three frequency bands variation over more than 20 dB re 1 μPa occurs, on a seasonal as well as sub-diurnal scale. The broadband SPL varies in a range of 21.97 dB for the Aural 66°S and 39.54 dB for the Aural 69°S. The broader range of SPL measured by Aural 69°S was likely the result of system noise. But also icebergs could have caused a broader variation of the noise, since Aural 69°S is located closer to the ice edge than Aural 66°S. The approximately sawtooth-like character of the annual variation is linked to the changing ice cover. In the 125 Hz third-octave band, strong differences to the trend of broadband SPL can be seen. This is the result of unidentified vocalisations between 100 and 400 Hz. by contrast, the 63 Hz third-octave band SPL is strongly correlated with broadband noise.

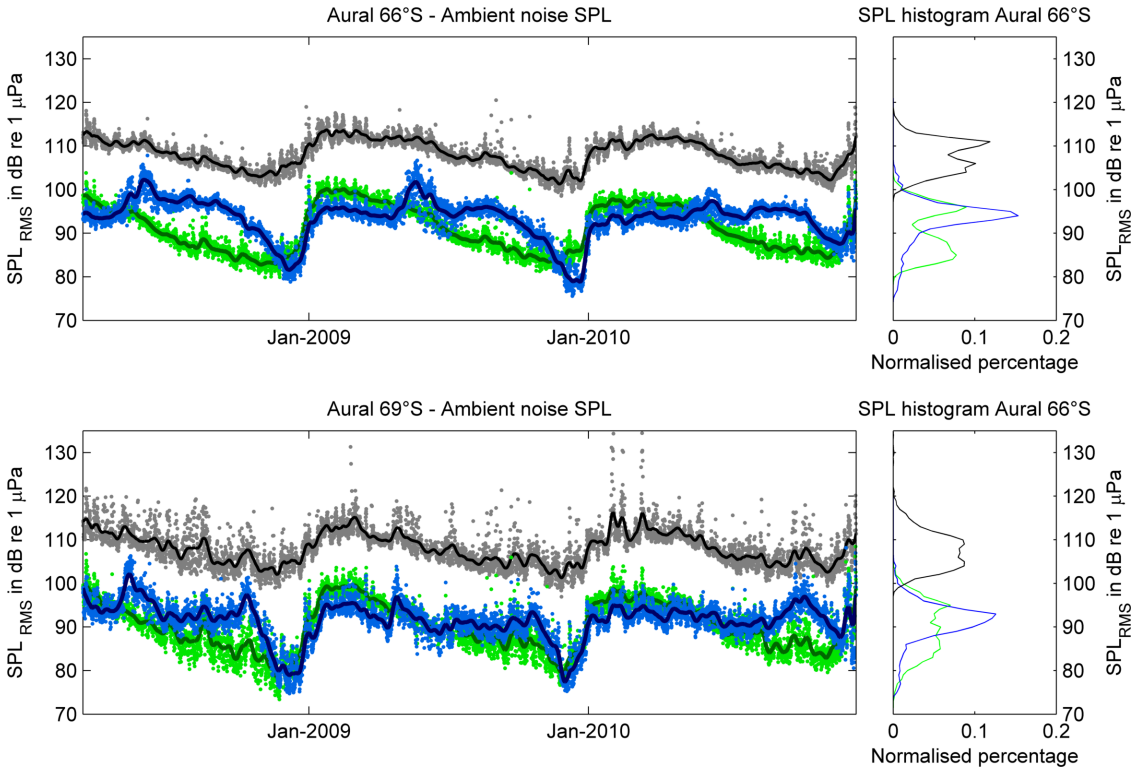

Figure 11: SPL_{RMS}in dB re 1 μPa values for each Aural averaged over the quietest 10 s per file. The upper plot represents data from Aural 66°S, the lower plot data from Aural 69°S. Continuous line represents a moving average filter with a window length of 7 days (42 files). The three graphs in each plot show SPL at different frequency bands: Grey = Broadband (10 - 16384 Hz), Green = third-octave band with center frequency 63 hz, Blue = third-octave band with center frequency 125 hz. Binsize of histograms: 1 dB re 1 μPa

For Aural 66°S the distribution of broadband SPL shows two distinct modes, the louder at about 111 dB re 1 μPa and the quieter at 106 dB re 1 μPa. The 63 Hz third-octave band behaves equally: The SPL values are distributed around two modes. But the 125 Hz third-octave band shows a different pattern, the values are spread around a narrow mode at 94 dB re 1 μPa for Aural 66°S, and 93 dB re 1 μPa for Aural 69°S. The recordings from Aural 69°S are much more diffuse. Here the broadband and 63 Hz third-octave band SPL values are spread less distinct around two modes: The louder at 109 db re 1 μPa and the quiter at 104 db re 1 μPa. The bimodal distribution of the broadband and 63 Hz third-octave band SPL, and the unimodal distribution of the 125 Hz third-octave band SPL seem to be the result of different processes.

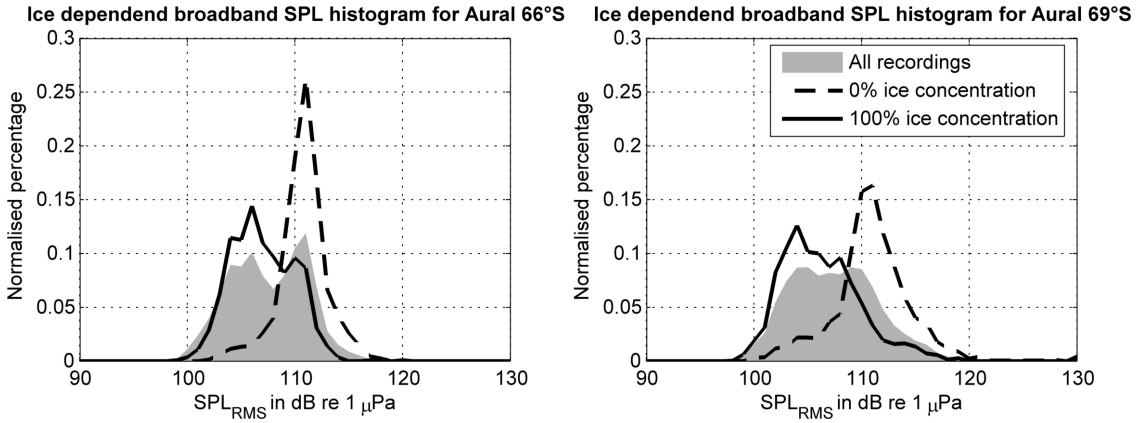

Figure 12: Histograms of broadband SPL under different ice conditions: All recordings histogram (grey area), histogram of recordings during open water above the recorder (broken line), histogram of recordings during full ice cover above the recorder (solid line). The left plot shows data from Aural 66°S, the right plot from Aural 69°S. Binsize of histograms: 1 db re 1 μPa. Histogram values were normalised by division with number of samples

The bimodal distribution of sound pressure levels can be explained considering the ice concentration above the recorder. In Figure 12 the distribution of the broadband SPL under different conditions is displayed as histograms. The grey area marks the distribution of all recorded SPL, the solid line only those during 100 % ice concentration above the recorder, and the broken line the distribution during 0 % ice cover. Clearly the distributions during 0 % and 100 % ice concentration behave very different. Whereas the SPL under open ocean conditions is distributed in a narrow peak around 111 db re 1 μPa for Aural 66°S and Aural 69°S, under ice cover conditions, SPL values are quieter and spread around a broad peak at 106 db re 1 μPa for Aural 66°S and 104 db re 1 μPa for Aural 69°S. Now the bimodal distribution of SPL values can be explained. It is a result of the two modes that define the Southern Ocean environment: open ocean conditions and ice covered conditions. Mean broadband SPL is 4 db re 1 μPa quieter during 100 % ice concentration than 0 % ice concentration for Aural 66°S and 5 db re 1 μPa Aural 69°S. The annual sea ice variation not only influences the ambient noise SPLs, but also impacts the power spectral density of the ambient noise.

5.2. Spectra

The frequency domain reveals broad spectral variation in the ambient noise. Figure 13 shows the mean spectra of different percentiles of the broadband SPL_{RMS}. The expected trend of lower spectral noise amplitudes at high frequencies is clearly visible. The loudest parts of the spectrum at both locations are peaks between 18 and 27 Hz. It is the loudest frequency band in the median spectrum of both recorders. The mean PSD of the narrow 27 Hz peak is 95 db re 1 μPa for Aural 66°S and 96 db re 1 μPa for Aural 69°S. The broader 18 Hz peak has a mean peak PSD of 97 db re 1 μPa for Aural 66°S and 96 db re 1 μPa for Aural 69°S. As will be discussed later in the text, this noise band is created by blue whales Z-calls (*Balaenoptera musculus*) and partly fin whale calls (*Balaenoptera physalus*) (Gavrilov et al., 2012, Širović et al., 2004). The sum of all calls creates a chorus. In this way, vocalising animals have a signature in the ambient noise.

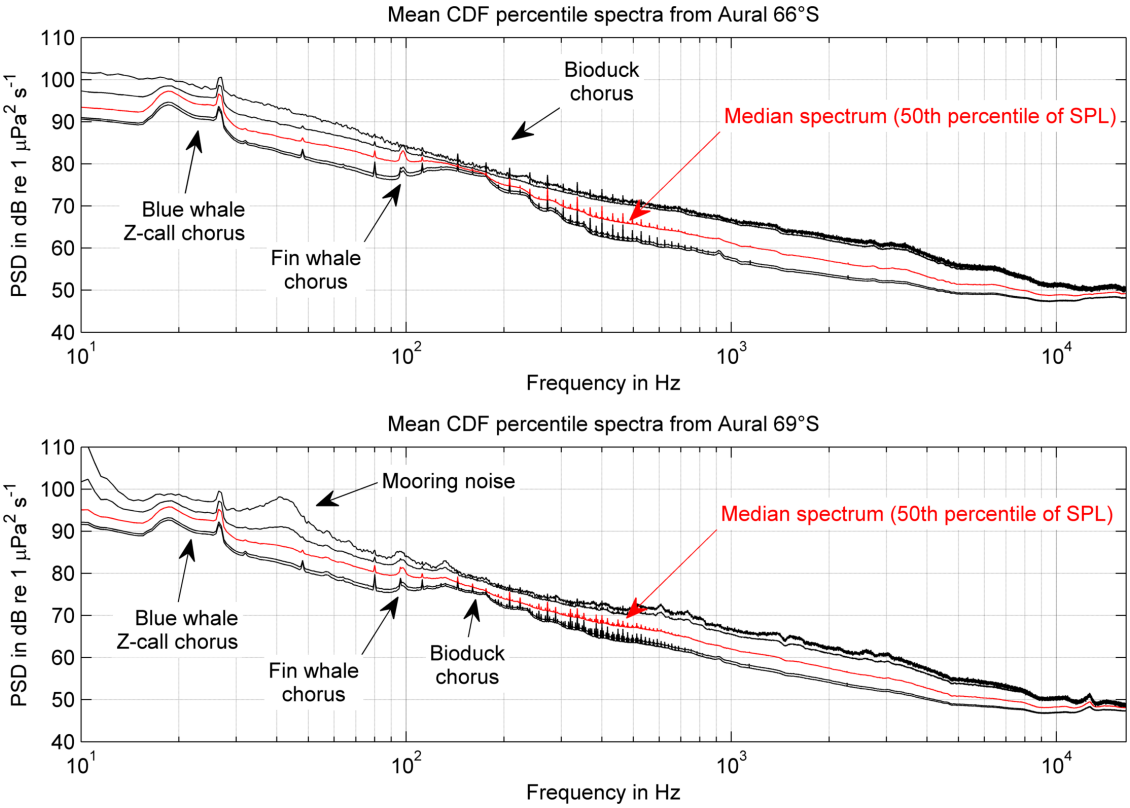

Figure 13: Mean spectra of percentiles of the cumulative density function for broadband SPL_{RMS} re 1 μPa. The 50th percentile is equal to the median spectrum (red line). The loudest 1 % of the recordings and the quietest 1 % show very distinct differences in their spectrum.

Another very prominent feature is a broad peak from 100 to 300 Hz. It is only visible during times where the SPL is quieter than the median SPL. This noise band is created by so called Bioduck sounds (Matthews et al., 2004). Their origin and character is still unknown, further information and analysis on the Bioduck sound will be presented in the discussion on sound sources. The narrow spikes visible from 40 to about 1000 hz are

electronic system noise and corresponding harmonics. The peak at 98 Hz is created by fin whales (*Balaenoptera physalus*). If we now compare the 2 diagrams some differences can be seen. The median Bioduck and fin whale chorus peaks are louder at 66°S than at 69°S: The median fin whale chorus is 83.1 db re 1 μPa for Aural 66°S and 81.4 db re 1 μPa for Aural 69°S. The median Bioduck chorus at 125 Hz is 80.4 db re 1 μPa for Aural 66°S and 78.8 db re 1 μPa for Aural 69°S. The strong peak from 30 to 50 Hz in the 90 % and 99 % percentile spectra of Aural 69°S is a result of noise created by the mooring itself. In the presence of currents unidentified loose part of the mooring created a banging broadband sound with maximum amplitude at 30 to 50 Hz.

The spectrum is strongly influenced by the ice cover. Figure 14 displays the mean spectrum during times of 0 % and 100 % ice concentration above the recorder. Except for the Bioduck peak from 100 - 300 Hz, between 10 - 16384 Hz the power spectral density is quieter during full ice coverage than no ice coverage. The Bioduck vocalisation is only present when there is an ice cover over the underwater recorders. In the high frequencies the spectra of both Aurals show slight ripples. These are possibly a created by the Aurals them selves. The exact frequency response of the recorders was not provided by the manufacturer, so parts of the spectrum could be amplified or attenuated.

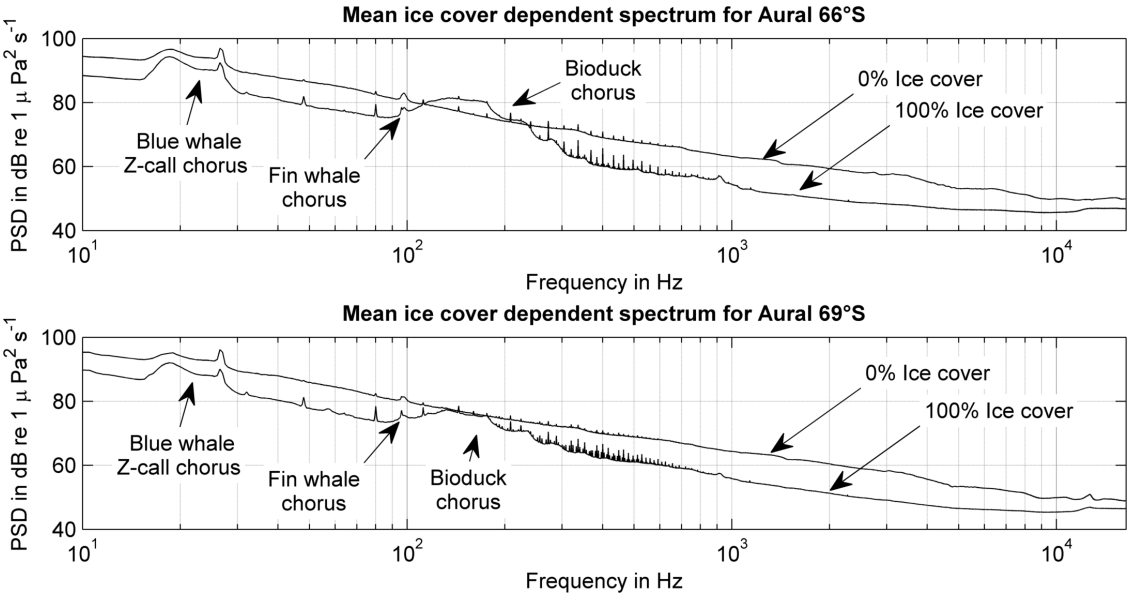

Figure 14: Mean spectrum of recordings during 0 % and 100 % ice concentration above the recorder. Upper plot for Aural 66°S, lower plot for Aural 69°S

The ambient noise subject to this thesis can be condensed and illustrated in the same manner as chosen by Wenz (1962). Figure 15 displays the averaged spectra of ambient noise in the Atlantic sector of the Southern Ocean under different conditions. It was created using the recording from Aural 66°S, since those from Aural 69°S contained too much system noise. The Matlab™ script to calculate and plot the figure is given in Listing 5 of Appendix C.

The difference between power spectral density ranges under ice cover and open ocean conditions become clearly apparent. Especially the wind influence on the spectrum changes dramatically when an ice cover is present. Wind speed increasingly influences the spectrum above 100 Hz under open ocean conditions: The difference between the PSD at 1 kHz from 0-9 m/s to 18-27 m/s wind speed is about 14 dB under open ocean conditions, and about 8 dB under ice cover conditions. Under the ice cover, frequencies above 500 Hz are increasingly influenced by wind speed.

In addition to noise created by physical processes, marine mammals contribute to ambient noise. The loudest noise band of lowest frequencies is produced by calling blue whales, displayed dark blue in Figure 15. The peak from 18 - 25 Hz is partly a signature of fin whales calls too. Blue and fin whale noise can best be distinguished by looking at the upper component of their calls. For the Antarctic population of blue whales, this is 26-27 Hz and for fin whales in the Atlantic sector of the Southern Ocean 98 Hz. In winter, the spectrum between 100 - 300 Hz is dominated by the Bioduck chorus. Since the exact time and frequency characteristics of the Bioduck call vary from year to year, only a frequency range can be given. In the mid and high frequency part leopard seals *Hydrurga leptonyx* seasonally influence the spectrum from about 270 - 370 Hz and crabeater seals *Lobodon carcinophagus* from about 400 - 1000 Hz.

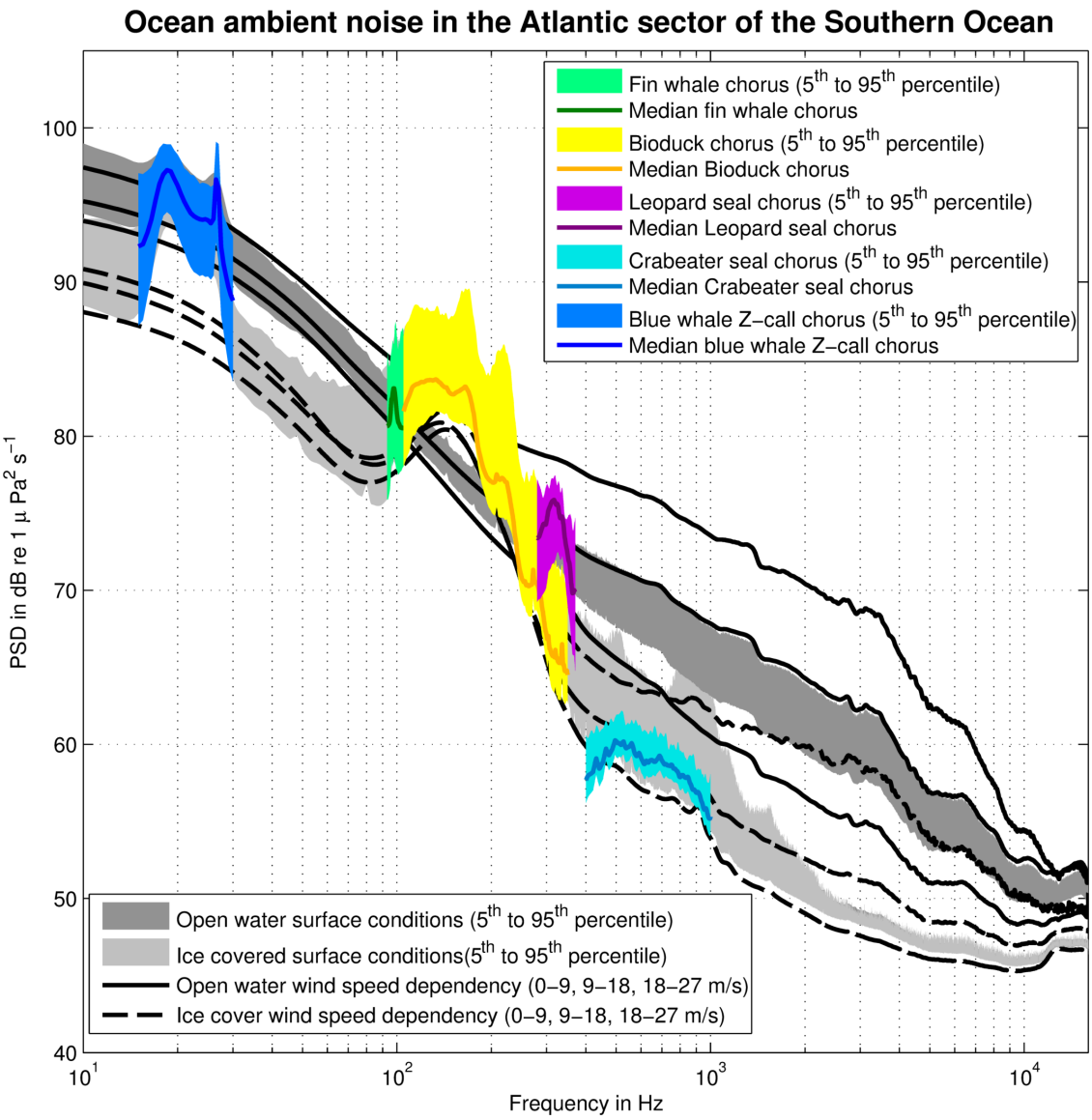

Figure 15: Overview of the continuous ambient noise present in the Atlantic sector of the Southern Ocean. Upper and lower boundaries of shaded areas are the mean spectrum of defined percentiles of the broadband SPL_{RMS}. Gray areas show broadband noise spectrum at open ocean conditions (Dark grey) and ice cover conditions (light gray). Black lines represent the spectrum averaged at 3 different wind speed intervals during 0 % ice cover (solid line) and 100 % ice cover (broken line). The coloured areas display noise bands characterised by marine mammal vocalisations, the solid line in these areas is the mean spectrum of the chorus. All spectra, except the marine mammal noise bands, have been smoothed using a low pass filter with a window length from 5 - 100 Hz.

5.3. Spectrograms

The SPL time series and averaged spectra alone do not provide sufficient information to understand the ambient noise dynamics of the Southern Ocean. To investigate the recordings both in spectral and temporal space, spectrograms were calculated. The ambient noise spectrogram was created by plotting the PSD of the quietest 10s per file as an image over time. Figure 16 and Figure 17 display the 3-year spectrogram as plot a), illustrating the entire variability of the ambient noise and depicting a strong difference between the ice free summer and ice covered winter period. The frequent broadband noise events and intense variations get damped by the ice cover during winter. Broadband noise is caused by wind and wave induced surface agitation. The wind speed at the Aural's locations underlies extreme variations, ranging from 0 to 27 m s^{-1}.

Plot b) of Figure 16 and 17 shows the variation of wind speed during the 3 year recording period and the broadband SPL. The increase and decrease of both curves fits together on scale of hours to days, but the seasonal changes in SPL can not be explained solely by the wind speed. The correlation of SPL with wind speed and ice is discussed in Section 6.1.1. Plot c) illustrates the ice concentration above each Aural and the mean daily solar radiation which drives the seasonal cycle. The combination of the plots illustrate the dynamics of the ambient noise.

The blue whale chorus is manifested between 18 and 27 Hz. In the spectrograms, the 26 - 27 Hz component is visible as continuous line and the diffuse 18 - 25 Hz component area underneath. The 26 - 27 Hz component is present year round, but changes in intensity. The broader and lower component (18 - 25 Hz) is present yearly from March to November. The 96 Hz fin whale chorus can be heard from May to June each year. During that time the PSD increases parallel in the 96 and 18 - 25 Hz band, the reasons for this is the structure of the fin whale call. Fin whale calls have two components: A lower one between 15 - 28 Hz and a higher component between 90 - 100 Hz (Širović et al., 2004).

A very prominent component of the ambient noise from May to November each year is the Bioduck chorus. It can yearly be seen in the spectrograms from about 100 - 300 Hz, although harmonics of the Bioduck chorus can create noise bands up to 1 kHz. In the recordings from both Aurals, year to year variation in the spectral structure of the chorus can bee seen. Although the frequency range stays the same, different bands are dominant in the vocalisations throughout each year. In the spectrogram from Aural 66°S the Bioduck chorus is loudest from May to October, whereas in the spectrogram from Aural 69°S the Bioduck chorus is less intense and loudest around May, than gets quieter and increases again in October. The characteristics of the Bioduck noise band will be analysed in the discussion.

During October and February the vocalisations of seals can be heard and a chorus detected in the background noise. From 400 to 1000 Hz crabeater seal vocalisations are part of the ambient noise in November and December. Their vocalisations are moans characterised by multiple harmonics (Klinck et al., 2010). Leopard seals produce very characteristic vocalisations from 200 to 400 Hz (Rogers et al., 1996), the chorus of this calls is most pronounced during December.

If we compare the spectrograms of Aural 66°S and Aural 69°S several observations can be made: The Bioduck noise band was present at different times. In the northerly Aural it was strongest in the beginning and mid of winter, when the ice cover reached its largest extent. In the recordings from Aural 69°S the Bioduck chorus could be heard at the end of winter, and in 2008 in the beginning of winter. The blue whale chorus reaches higher amplitudes in the northern Aural. Also the fin whale chorus reaches higher levels at that location. The spectrogram from Aural 69°S is much noisier than those from Aural 66°S. This seems to be the result of system noise created by the mooring and the recorder. Knocking sound frequently occurred, also overdrive noise caused by vertical displacement of the hydrophone was recorded. The thin lines visible in the Spectrograms are artefacts of electronic noise produced by the recorder.

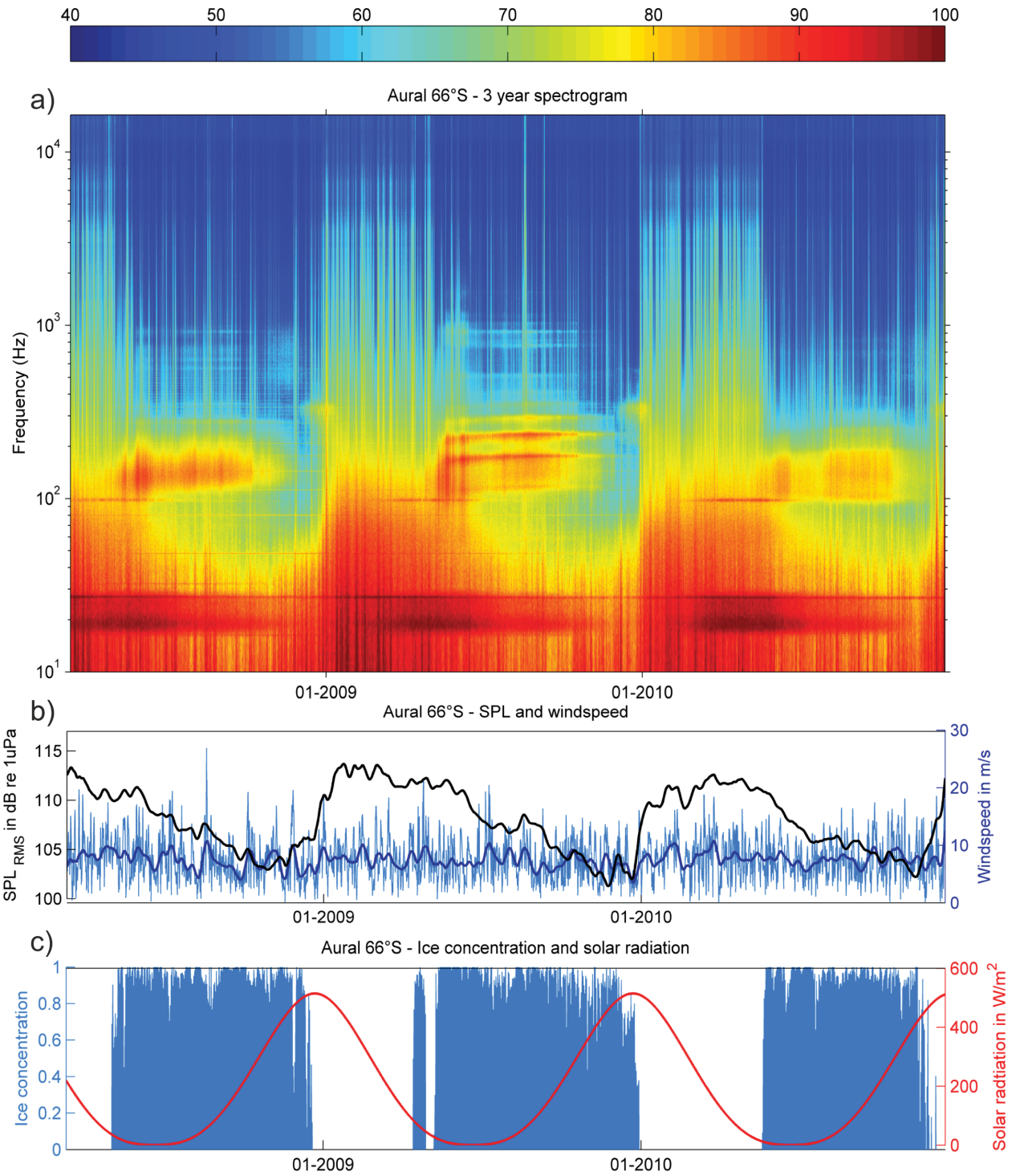

Figure 16: 3 year plot of the time and frequency characterisitics of the ambient noise and correlating physical parameters at 66°S. a) Spectrogram of ambient noise, generated by plotting PSD of quietest 10 s window over time, Colour bar shows the PSD in db re 1 μPa^2 s^{-1}, b) Plot of broadband SPL (black, with moving average filter of windowlenght 7 days) and wind speed (light Blue: 6 h interval, dark blue: wind speed with moving average filter of windowlenght 7 days), c) Ice concentration (blue area) and solar radiation (red) in 6h interval

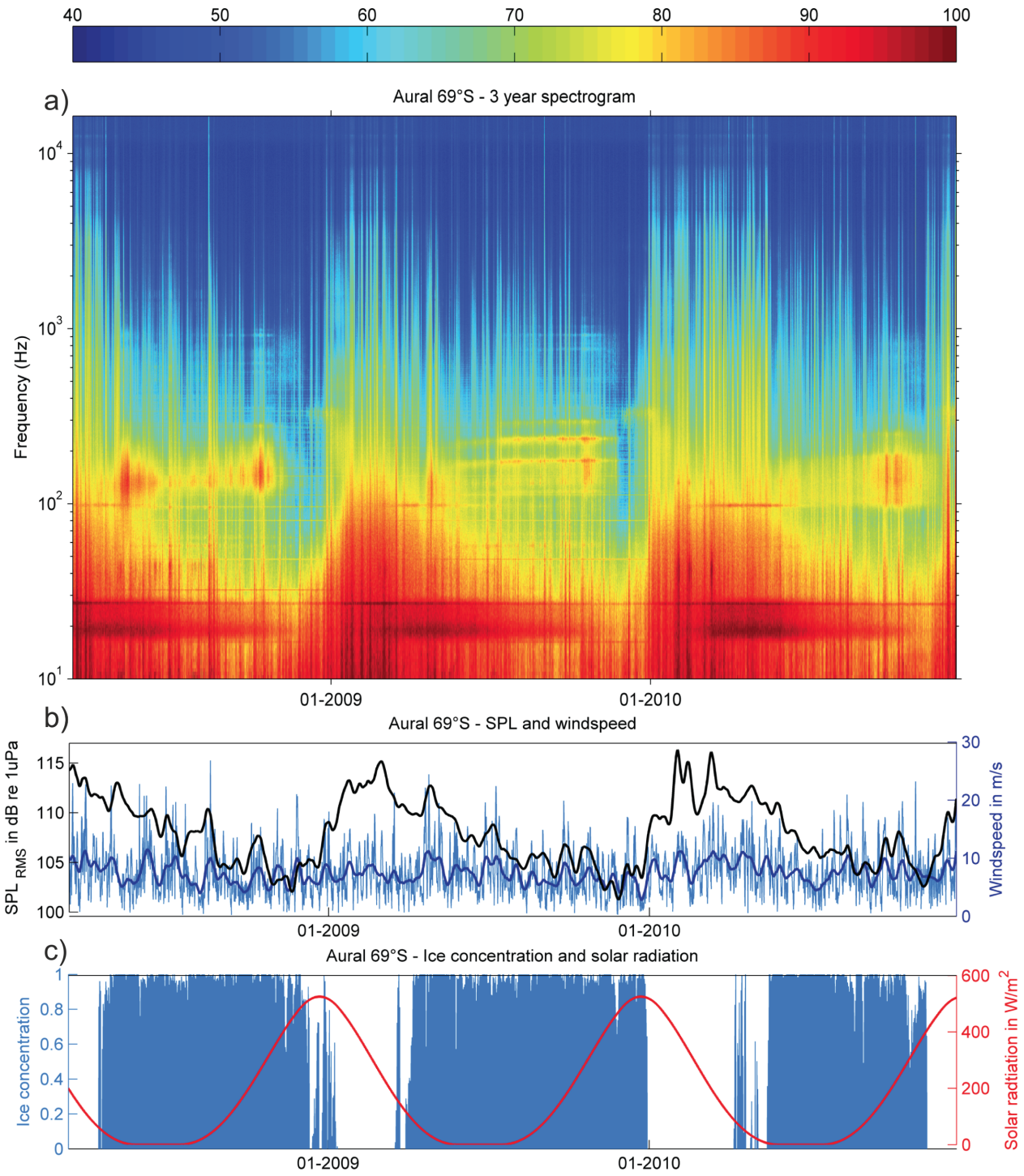

Figure 17: 3 year plot of the time and frequency characterisitics of the ambient noise and correlating physical parameters at 69°S. a) Spectrogram of ambient noise, generated by plotting PSD of quietest 10 s window over time, Colour bar shows the PSD in db re 1 μPa^2 s^{-1}, b) Plot of broadband SPL (black, with moving average filter of windowlenght 7 days) and wind speed (light Blue: 6 h interval, dark blue: wind speed with moving average filter of windowlenght 7 days), c) Ice concentration (blue area) and solar radiation (red) in 6h interval

6. Discussion

6.1. Sound sources

6.1.1. Physical sound sources

A major source of broadband noise in the world's oceans is surface movement. This applies to the Southern Ocean as well. What distinguishes the Southern Ocean is a seasonally present ice cover, which attenuates the surface agitation and dampens the ambient noise. Surface waves are mainly excited by wind blowing over the sea surface. Thus ambient noise sound pressure level correlates very well with wind speed. The scatter plots of wind speed and broadband SPL_{RMSs} in Figure 18 exhibit two clusters. In the scatter plot from Aural 66°S the clusters can be clearly distinguished, for the southerly Aural the scatter plot is much more diffuse. This is a result of system noise in the recordings. The upper cluster from 66°S, marked in red, suggests an approximately linear relationship between wind speed and sound pressure level. The formation of the two clusters is a result of sea ice. The red upper cluster represents open ocean conditions, the lower cluster ice covered conditions. The two modes of ambient noise in the Southern Ocean are:

- Open water mode (January to June)
- Ice cover mode (July to December)

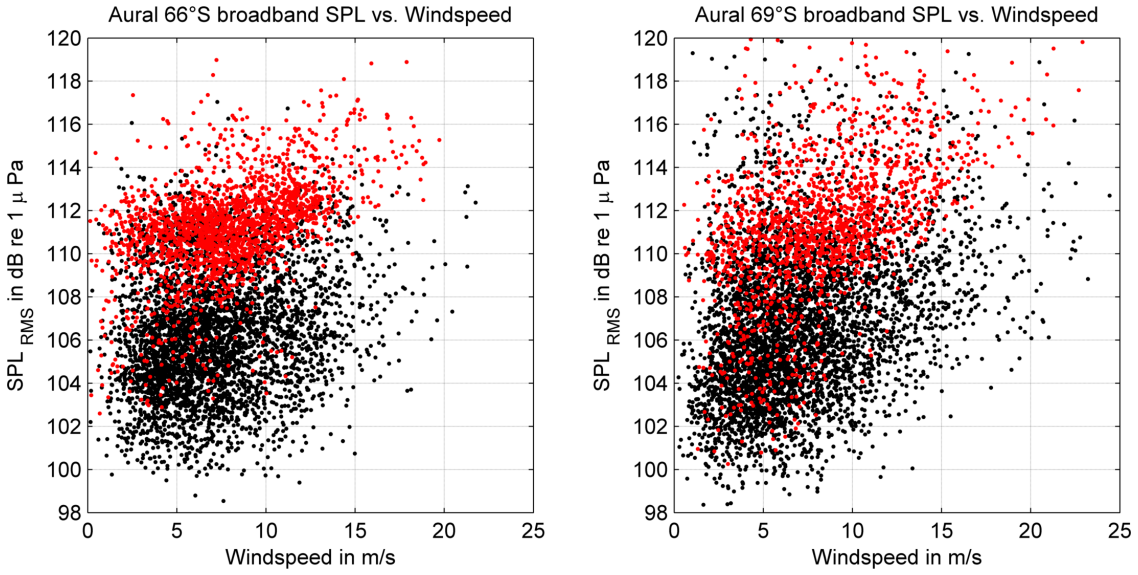

Figure 18: Scatter plot shows relationship between wind speed and broadband SPL db re 1 μPa, left plot for 66°S and right plot for 69°S. Red points represent SPL values during 0 % ice cover

The histograms of broadband SPL under different ice conditions in Figure 12 confirms this notion. The histogram, especially pronounced for Aural 66°S, shows two distinct modes that are attributed to open water and ice covered conditions. In the beginning of

Antarctic winter the sea ice cover increases until it reaches its maximum extent in September (Cavalieri and Parkinson, 2008). This increasingly dampens the ambient noise. From December onwards the ice cover disintegrates and the SPL reaches open ocean values again. This explains the sawtooth like pattern (Figure 11) of SPL over the three year recording period. The yearly cycle can also be seen in the spectrograms of ambient noise in Figure 16 and 17.

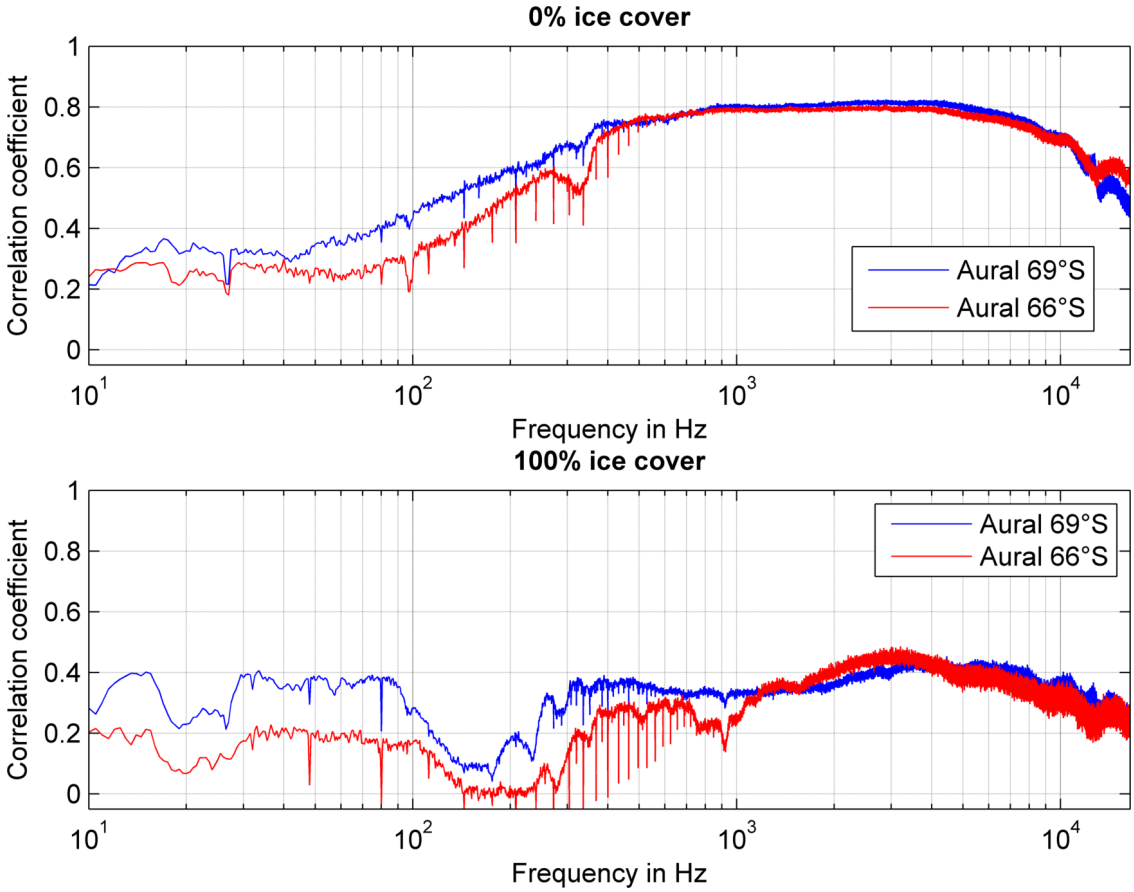

Figure 19: Frequency dependence of the correlation coefficient between broadband SPL and wind speed. The upper plot shows open ocean conditions, the lower plot ice cover conditions. The colours indicate the two recorders. Generated using example Matlab™ code in Listing 4

In Figure 19 the frequency dependence (using Pearson's correlation coefficient) of the correlation coefficient between broadband SPL and wind speed, under open ocean and ice cover conditions is displayed. The plot was generated by correlating the wind speed time series with each power spectral density time series from 10 - 16384 Hz (PSD of the quietest 10 s per recording using Welch's method in 0.5 Hz bins). A significant difference between the two modi is apparent. During 0 % ice concentration, frequencies above 100 Hz correlate well with wind speed, with a correlations coefficient up to 0.8. This confirms the results of Wenz (1962). Under 100 % ice concentration the correlation coefficients are low over the full spectrum, reaching values around 0.4. In both plots,

distinct frequency bands with a reduced correlation can be seen. This is a result of marine mammal vocalisations, the blue whale and fin whale band, as well as the Bioduck band show less correlation with wind speed, than regions of the spectrum that are not influenced by animal vocalisations. The narrow spikes visible in the spectra are artefacts caused by system noise.

6.1.2. Biological sound sources

Blue whales:

The loudest band in the continuous ambient noise spectrum is created by blue whales (*Balaenoptera musculus*) vocalisations. These largest of baleen whales produce sounds named Z-calls in the frequency range from 18 - 27 Hz (Sirović et al., 2007). The spectrogram of a typical Z-call is shown in Figure 20. It's spectrogram resembles a Z and consists of two parts, an upper part between 26 - 27 Hz followed by a down sweep to an 18-20 Hz component. This call is typical for the Antarctic population of blue whales, different populations can be allocated by their typical vocalisations (Mcdonald, 2006). The exact purpose of these calls is still unknown, although they probably have a social function. The chorus created by these calls are displayed in Figure 21. A comparison of the noise bands reveals that the chorus is stronger in the recordings of the northern Aural. This agrees with the assumption that blue whales are attributed to open water and avoid the ice cover.

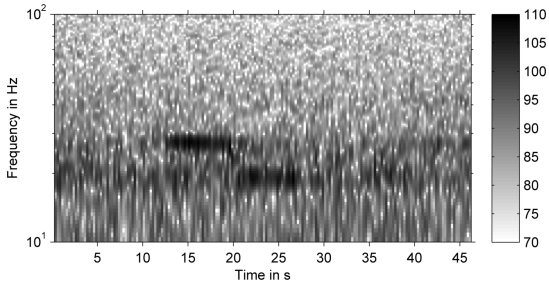

Figure 20: Blue whale Z-call, typical for Antarctic blue whale population, FFT size: 16384 , Overlap: 8192, colour bar shows the PSD in db re 1 μPa^2 s^{-1}

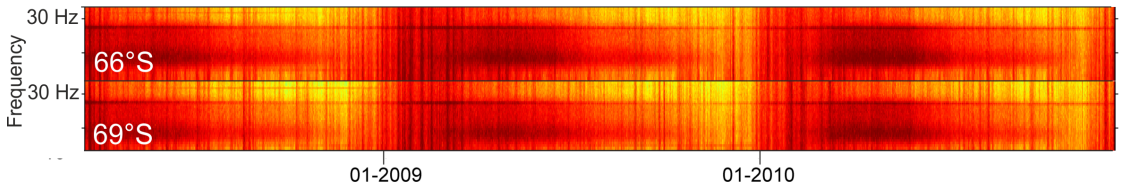

Figure 21: Comparison of blue whale chorus noise bands, Upper plot for Aural 66°S and lower for Aural 69°S, derived from Figure 16 and 17, colour shows the PSD in db re 1 μPa^2 s^{-1}

In a two day study McDonald et al. (2001) observed that only male blue whales emit calls and their source level can be up to 188 dB re 1μPa. Another interesting aspect of these calls is their frequency development over years. The frequency of the upper Z-Call component is continuously decreasing, with a decline of 0.05 Hz per year in the Southern Ocean (McDonald et al., 2009). Gavrilov et al. (2012) confirmed the frequency decrease for Antarctic blue whales and reported an inter annual variation in the Z-call frequency.

This was also observed in the ambient noise data from Aural 66°S and 69°S (see Figure 22). During the 3 year recording period the upper Z-call component decreased from 26.8 Hz in 2008 to about 26.7 Hz in 2009 and 26.6 Hz in 2010 (measured as mean over each year). So far, no explanation for the frequency decrease has been confirmed. Theories on the origin and purpose of the down shift reach from sexual selection to popular song trends.

It is estimated that now 1700 blue whales belong to the Southern Ocean blue whale population (Perrin et al., 2009). During industrial whaling in the early 20^{th} century about 325,000-360,000 blue whales were caught (Perrin et al., 2009). Branch et al. (2004) estimated the pre-whaling stock of Antarctic blue whales to be 239,000 individuals. Considering the noise band produced by the contemporary population, blue whale chorus band levels might have been 20 dB higher before the depletion of stocks.

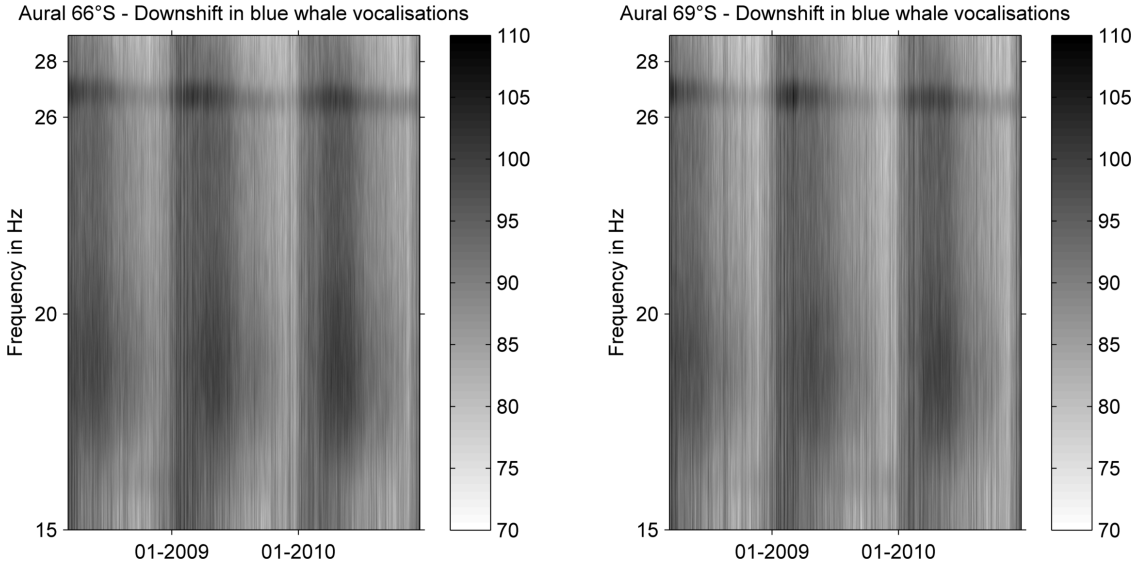

Figure 22: Downshift in blue whale vocalisation frequency. The left side displays analysis from Aural 66°S, the right from Aural 69°S, FFT size: 3276800 which results in a frequency resolution of 0.01 Hz, colour bar shows the PSD in db re 1 μPa^2 s^{-1}

Fin whales:

The second baleen whale species influencing the noise spectrum are fin whales . They are less endangered than blue whales. It is estimated that approximately 15200 fin whales roam the Southern Ocean (Perrin et al., 2009). The population present in the Atlantic Sector of the Southern Ocean vocalises at two frequency bands: Between 15 – 28 Hz and in a pronounced frequency band around 98 Hz. In both Aurals the choruses created by the 98 Hz calls are clearly visible. The 15-28 Hz component of the fin whale chorus overlaps with the blue whale chorus and can not be clearly distinguished. But in the 3 year ambinet noise spectrogram of Figure 16 and 17 a rise in the 15-28 Hz band parallel to the 98 Hz calls can be seen. The upper vocalisation frequency is actually

somewhat higher than measured by other scientist off the Antarctic peninsula: Sirović et al. (2007) reported that the upper component of Antarctic fin whale call is centred around 89 Hz. The reason for this difference is not known, but a possible explanation is regionalism in fin whale call type. Distinct populations may have evolved typical calls. If this is the case, acoustic monitoring of the fin whale chorus could be used to differ between several populations.

A comparison of fin whale chorus strength can be seen in the spectrograms of Figure 24. The fin whale chorus can bee seen as thin line at 98 Hz. In the recordings of the northern recorder, the fin whale chorus reaches louder band levels and duration than in those from Aural 69°S. This fits to the findings that fin whales like temperate to cold open waters and avoid sea ice (Perrin et al., 2009). The fin whale chorus can be heard less on the location of Aural 69°S, because the ice cover there lasts longer.

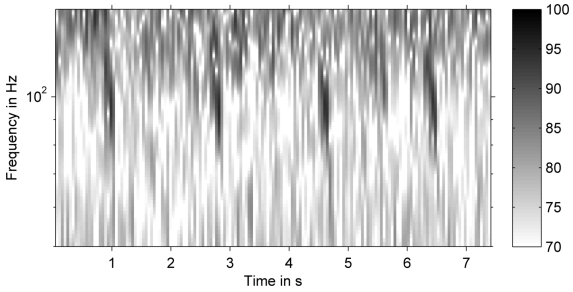

Figure 23: 98 Hz component of finwhale calls, FFT size: 3000, Overlap: 8192, Colour bar shows the PSD in db re 1 μPa^2 s^{-1}

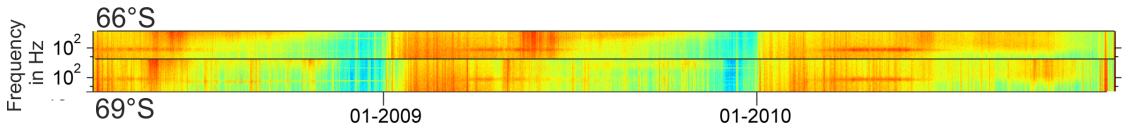

Figure 24: Comparison of fin whale chorus, upper plot for 66°S and lower plot for 69°S. colour shows the PSD in db re 1 μPa^2 s^{-1}, colour scale equals those from Figure 16 and 17. Fin whale chorus is thin line at 98 Hz.

Seals and other mammals:

Crabeater seal noise was recorded from the end of September to the end of November in Aural 66°S and from mid September to the end of November in Aural 69°S. In 2009 no Crabeater seal noise was recorded with Aural 69°S. The typical calls cover a frequency range from 260-2500 Hz and 1000-4900 Hz (Klinck et al., 2010). The crabeater seals noise present in the recordings ranges from 500-1000 Hz, here lies the main spectral energy of the abundant low moan calls. It is shown here that it is possible to monitor the occurrence of crabeater seals using the noise band they produce.

The same holds for leopard seals, whose vocalisations are extremely abundant from the beginning of December to mid January in Aural 66°S and Aural 69°S. They produce a very pronounced noise band between 300 and 400 Hz (Rogers et al., 1996). The timing of the seal choruses confirms the seasonality of seal vocalisations investigated by Van Opzeeland et al. (2010).

Other species of marine mammals could also be identified in the recordings. Transient vocalisations of weddell seals and ross seals were audible. The echolocation clicks of sperm whales and killer whales were frequently present in the recordings, also humpback whales calls were recorded. However, these vocalisations do not produce a significant band in the ambient noise spectrum and were not analysed in this thesis.

6.1.3. The Bioduck sound

One of the most dominant sounds recorded in winter were the Bioduck calls. These signals of unknown origin dominate the spectrum from 100 to 300 Hz from May to November each year. The sound was recorded by both Aurals, although presence varied in intensity (see the spectrograms in Figure 16 and 17). The different intensities suggest that the sound source is moving during the winter. In the beginning of winter it is intenser in the recordings from Aural 69°S and in mid winter, when the sea ice cover reaches its largest extent, it is most intense in the northern Aural. At the end of winter it can be heard in Aural 69°S again. This suggests that the Bioduck sound source could be attributed to the ice edge region.

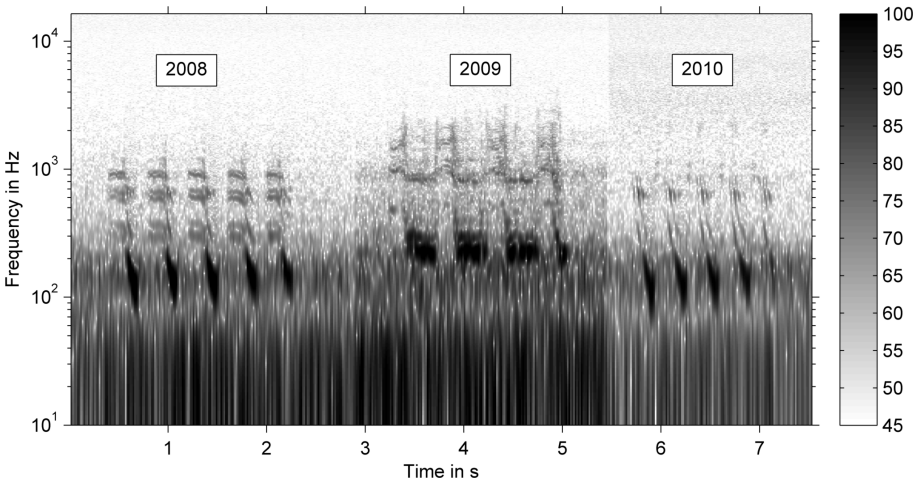

Figure 25: A comparison of Bioduck calls recorded during by the aurals, FFT size: 2048, Overlap: 1024, colour bar shows the PSD in db re 1 μPa^2 s^{-1}

Figure 25 shows the spectrogram of 3 different Bioduck calls. It consist of a repeated series of sweeps and grunts in the form of a pulse train from 100 to 3000 Hz. The modulation and structure of the call changes from year to year, but the rough frequency and time characteristic stay the same. The intervals between the pulse trains stay the same each year. There are several types of Bioduck calls, different in number of sweeps and grunts per call and speed of the pulse train. The frequency range stays the same for the different call types.

A possible source for the Bioduck sound is the vocalisation of Antarctic minke whales (*Balaenoptera bonaerensis*). These baleen whales are known to overwinter under the Antarctica sea ice. They are possibly affiliated to the ice edge region. Cetacean distribution studies sighted minke whales both in open and ice covered water. Most studies were

conducted in open water, so the distribution of minke whales in the sea ice and ice edge region is not sufficiently studied (Thiele et al., 2000). Their vocalisations have not been extensively studied yet. But the vocalisations of the northern minke whale (*Balaenoptera acutorostrata*) are well studied and cover roughly the same frequency range as Bioduck calls (Gedamke et al., 2001, Mellinger et al., 2000).

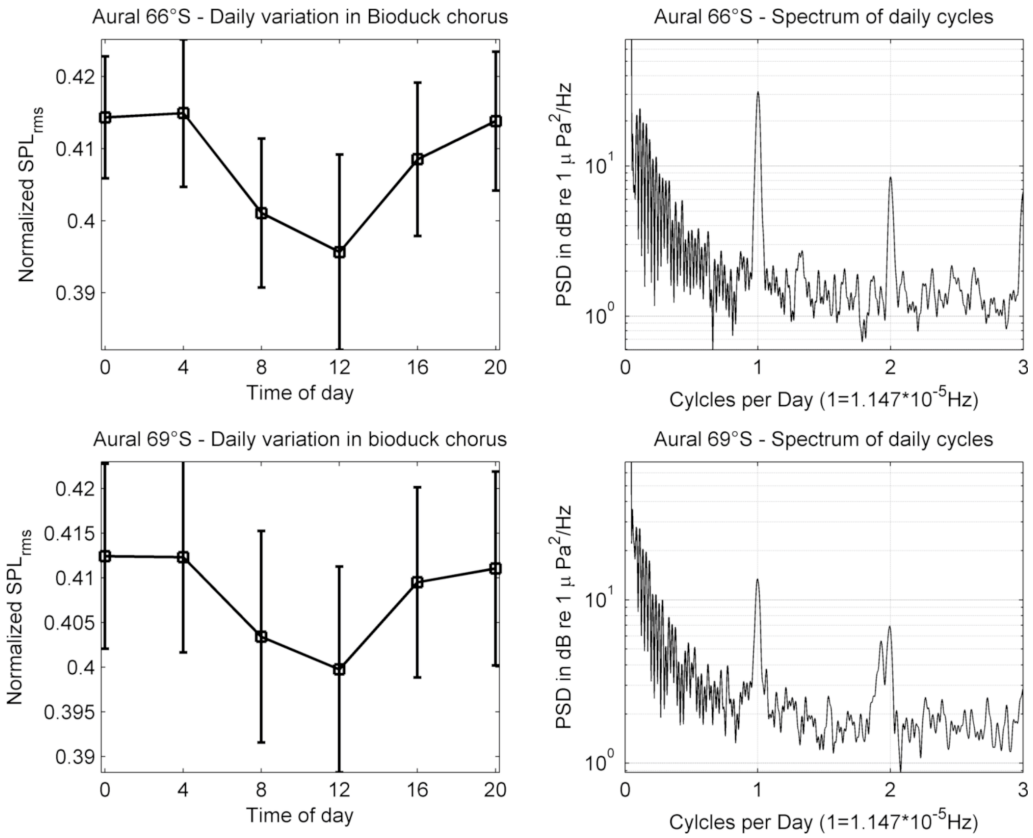

Figure 26: Analysis of the diel pattern in the Bioduck chorus. The upper box shows analysis for Aural 66°S and the lower box for Aural 69°S. Left plot shows averaged daily variation of the 125 - 150 Hz frequency band from May to July, from 2008 to 2010. Errorbars show standard deviation. The right spectrum is a plot of the power spectral density (FFT size = 262144) after Welch of the 125 - 150 Hz frequency band from May to November, from 2008 to 2010

A closer analysis of the Bioduck noise band revealed a diel pattern in the recordings (see Figure 27). The amplitude of the Bioduck chorus follows a circadian rhythm (exactly 24 h), this rhythm is developed strongest from early May to late July each year, in the beginning of Antarctic winter. The occurrence of daily cycles in the Bioduck band can be seen in Figure 28 and the daily variation of SPL_{rms} and the corresponding spectrum of daily cycles in Figure 26. As displayed in the spectrogram in Figure 28, the oscillation is not equally strong each year, but present at the location of both recorders in the beginning of winter. Figure 27 shows an example of the circadian Bioduck rhythm from May to July 2008. The oscillation can be seen in the SPL plots and spectrograms. This oscillations occurs because the sound sources (possible minke whales) either: Call less, call quieter

or migrate to another region.

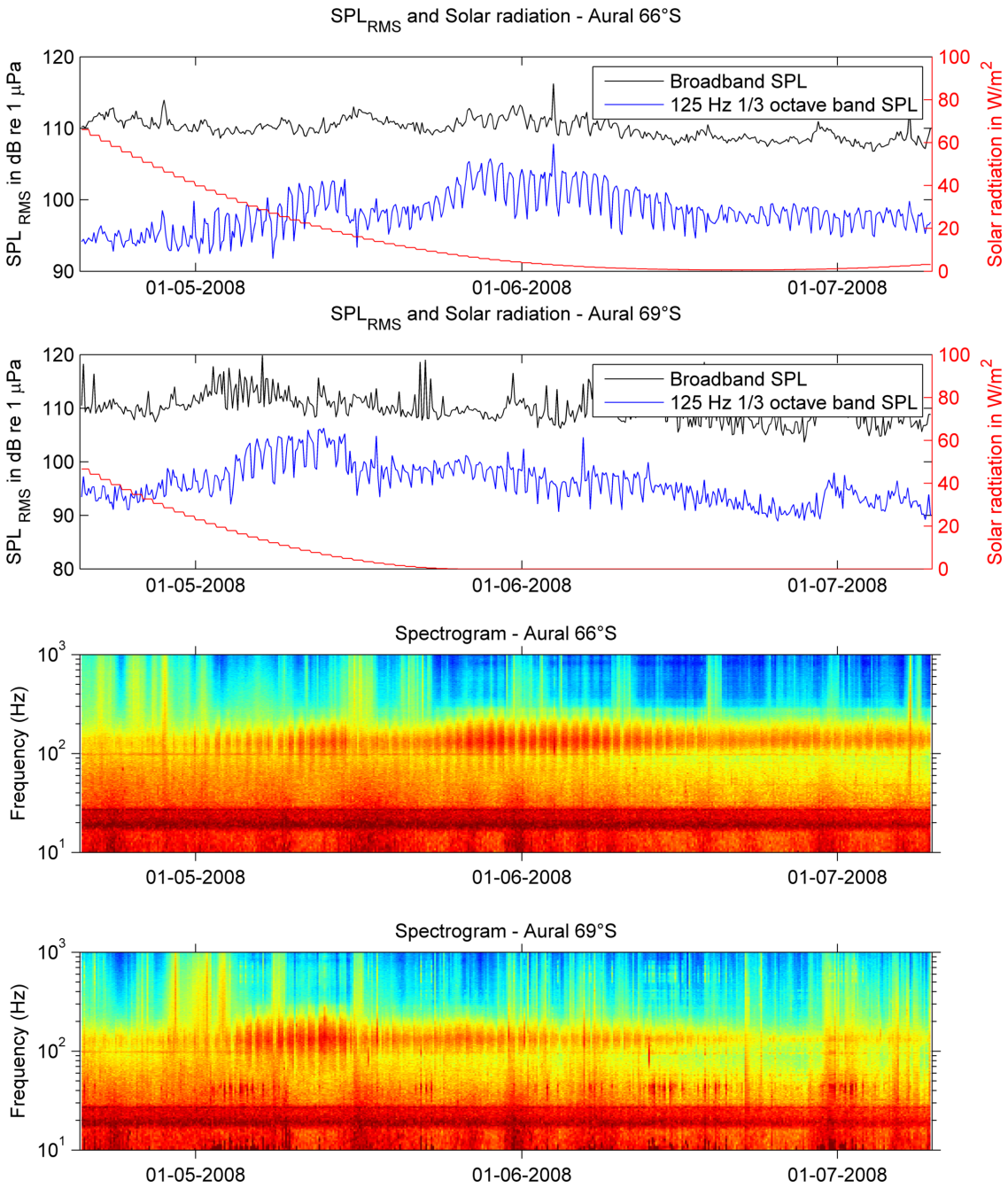

Figure 27: Example of diel pattern in Bioduck chorus, from 15^{th} April to 15^{th} July 2008. The upper two plots show the broadband and 125 Hz third-octave band SPL over time (Black and blue lines). Additionally the mean daily solar radiation is plotted in red. The lower two plots show the spectrogram of the ambient noise, colour shows the PSD in db re 1 $\mu Pa^2\ s^{-1}$, scale is the same as for the 3 year spectrograms in Figure 16 and 17. The oscillation of the Bioduck chorus is visible in the spectrograms of both Aurals, between 100 and 300 Hz.

What makes this fact surprising is, that the sun does rise above the at the location of Aural 69°S from mid may to mid July, and only reaches the horizon during that period at Aural 66°S's location. Still the Bioduck chorus follows a circadian rhythm, even in times of nearly 24 darkness. Only at noon twilight illuminate the under ice habitat. What ever triggers the daily rhythm must be partly independent from the solar cycle. The internal clock of many animals can be independent from sunlight. If we assume Antarctic minke whales to be the source of Bioduck calls, three hypothesis can be developed.

The first is, that the internal clock of Antarctic minke whales themselves follows a circadian rhythm, and they alter their vocalisation behaviour according to their inner clock. The second possibility is that Antarctic Minke whales alter their behaviour according to the circadian vertical migration of krill.

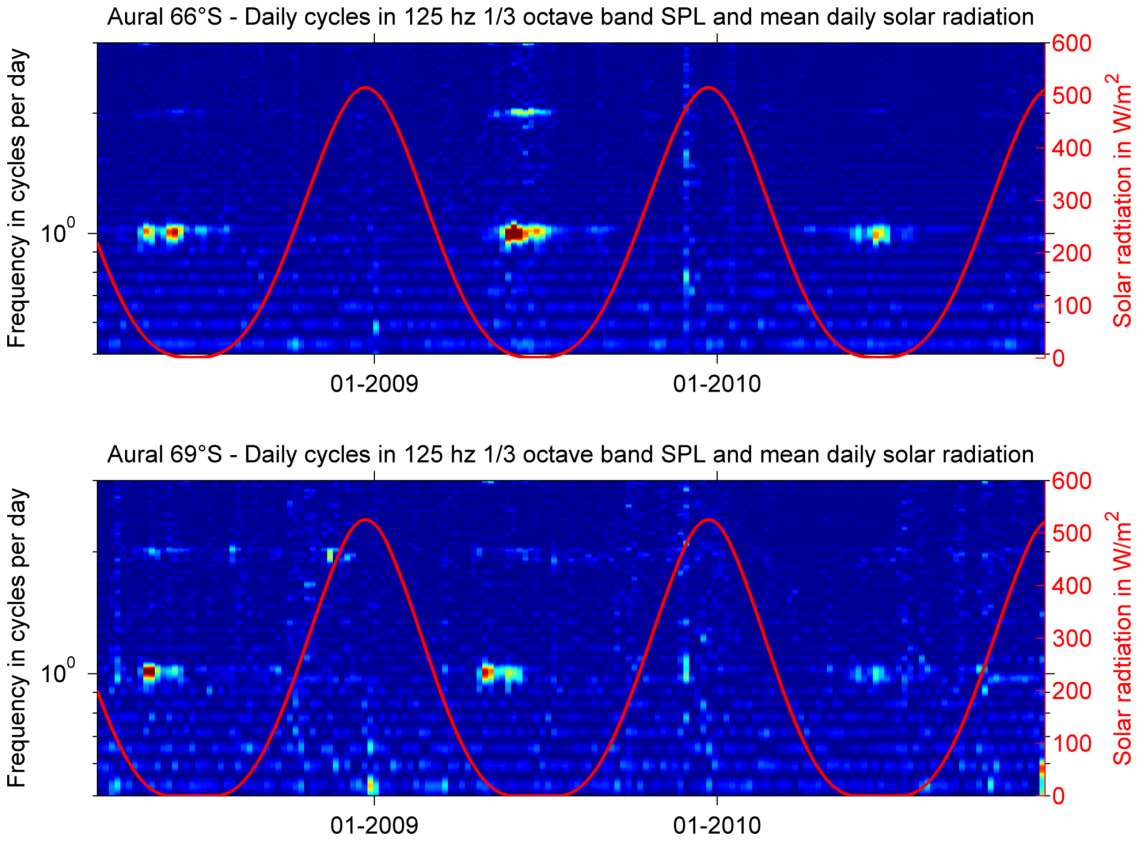

Figure 28: Spectrogram of daily cycles in Aural 66°S (upper plot) and Aural 69°S (lower plot), the colour scale of reaches from 0 to 50 db re 1 μPa (blue to red). The red line indicated solar radiation

Many species of the plankton show a diel vertical migration. This has the advantage of exploiting abundant food sources at the surface during night, and escaping from predators into deeper water layers during day. The vertical migration of Antarctic krill (*Euphausia superba*) has been studied in controlled experiments and field observations. Studies in laboratory tanks by Gaten et al. (2008) showed that Antarctic krill keep an approximately circadian rhythm in total darkness. Teschke et al. (2011) proposed that Antarctic

krill posses an endogenous circadian timing system that is linked to the krills metabolic rhythms. During two expeditions with RV Polarstern Flores et al. (2012) sampled Antarctic krill near the Greenwich meridian transect. Their observations in Antarctic winter showed a strong difference between day and night time catches of krill in the surface layer. During daytime nearly 0 individuals per m^2 were caught, but at night up to 20 individuals per m^2. During summer, the phase switched and krill was increasingly caught at the surface during daytime. Antarctic krill is the main food source of Antarctic minke whales (Ichii and Kato, 1991). Assuming that the Antarctic minke whales vocalisation and feeding behaviour is connected, the circadian vertical migration of Antarctic krill can explain the circadian rhythm in the Bioduck noise band.

That Antarctic krill is the origin of the Bioduck signal is unlikely. This species has been subject to extensive studies, in field observations as well as laboratory experiments. No vocal behaviour has been reported for Antarctic krill so far.

A third hypothesis is that the Antarctic minke whales use the little light left during Antarctic winter to find regions with a thin or no ice cover. These whales have to find holes or thin patches in the ice cover to breathe. How they sense this is unknown yet. It is possible that the Bioduck vocalisations are used as echolocation signal. The diel variation could occur because the need to echolocate is less during midday because the whales can use the remaining light to find breathing holes. But this does not explain the seasonal distinctness of the circadian rhythm.

6.1.4. Anthropogenic sound sources

During the 3 years recording time, no shipping noise, except from the RV Polarstern during deployment and recovery of the Aurals, could be identified. This is a result of the remote location of the recorders. Severe storms, pack ice, the risk of icebergs, as well as the lack of human settlements and industries along its boundaries reduce the number of ships crossing the Atlantic sector of the Southern Ocean. This can clearly be seen in the map of global shipping intensity in Figure 7. The Southern Hemisphere remains less travelled than the Northern Hemisphere and except for research and cruise vessels, few ships operate off the coast of Antarctica.

6.1.5. System noise

The recordings of Aural 69°S were severely influenced by system noise from the mooring and recorder. This noise was possibly caused by the shearing of the mooring through currents. A tidal oscillation could be identified in the system noise (see Figure 26). Two types of noise ocurred: Knocking sounds created by loose parts of the mooring equipment and overdrive created by pressure change due to vertical displacement of the hydrophone. In Figure 29 the distribution of depth values from Aural 66°S and 69°S is shown as histogram. Aural 66°S was moored stable and only experienced a depth change within a 4 m range. Aural 69°S fluctuated more in depth, within a range of 15 m. The reason for this could be the design of the mooring and the currents at the location of the mooring. Above Aural 66°S only 1 steel and 2 Benthos flotations were located, above Aural 69°S an additional heavy upward looking sonar was attached. This might have introduced instability to

the mooring. Alternatively, the current strength was stronger at the location of Aural 69°S.

The electronic recording and storage modules of the Aurals produced distinct narrow spikes in the spectrum. These are present with multiple harmonics and are typical electronic noise, fortunately their PSD is quiet low. However, during quiet ice covered time these lines become visible in the spectrum and spectrogram.

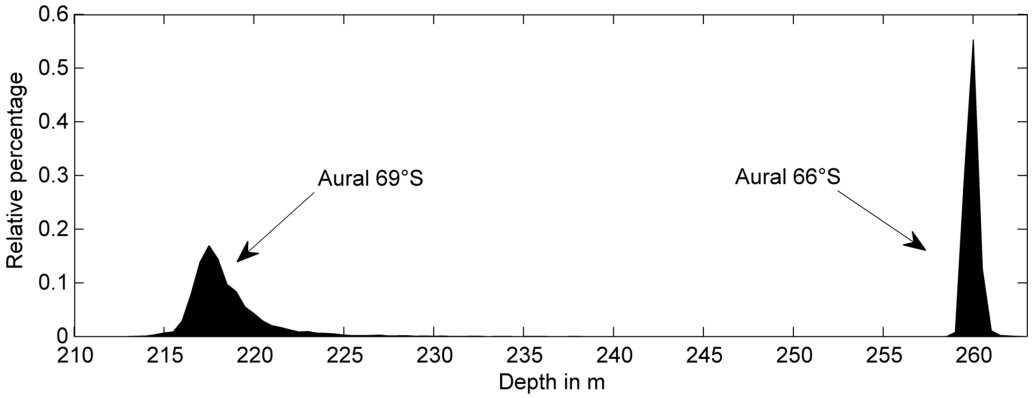

Figure 29: Histogram showing the distribution of depth for Aural 66°S and 69°S

6.2. Ambient noise dynamics

The variation present in the ambient noise of the Southern Ocean is caused by multiple cycles, from large scale seasonal changes of sea ice to hourly variation in sea state and wind speeds.

With the growth and melting of the sea ice cover, the soundscape changes between two acoustic ambient noise modi: Open ocean noise and quieter ice covered ocean noise. Between the two states, times of transitions occur, varying in duration and prevailing noises. The earth's movement around the sun and the angle of the earth axis results in seasonal changes of the solar radiation at the earth's surface. In the polar regions, this leads to seasonal variation of the sea ice extent and periods of persistent sunlight or darkness. This process is the main driver of the annual large scale variation in ambient noise. In Antarctic winter, when the sea ice extends up to $18.9 \cdot 10^6 \text{km}^2$ (Cavalieri and Parkinson, 2008), broadband noise levels are at average 4.25 dB quieter than during summer, when there is no sea ice present. Also the spectral distribution of the noise changes. The sea ice dampens the surface waves and leads to quieter noise levels, especially in frequencies above 1 kHz. This can be seen in the spectrum of Figure 15. The distance between the ranges of the prevailing noise is considerably larger above 1 kHz. A possible explanation is that noise under the ice cover is produced by waves in ice free regions further away, and movements and collisions of ice floes. Absorption and scattering result in increasing attenuation of higher frequencies. The sea ice can be seen as low pass filter.

Ambient noise also varies on a scale of days and hours. This is the direct variation of the wind and wave field above the observer. High and low pressure systems frequently pass the Southern Ocean. The Southern Ocean is famous for it's fierce storms, in which

wind speeds up to 27 m/s were reached at the locations of the Aurals. This is reflected in the underwater soundscape, since storms create loud underwater noise. The many spikes of the SPL plot and in the 3 year spectrogram are caused by passing storms.

Diurnal and sub-diurnal oscillations are apparent in the ambient noise. Tidal noise was identified in the recordings from Aural 69°S. Loose parts of the moorings produced system noise, partly with a frequency of about 1.8 cycles per day. The unidentified Bioduck calls produce a noise band that shows a circadian rhythm in the beginning of Antarctic winter.

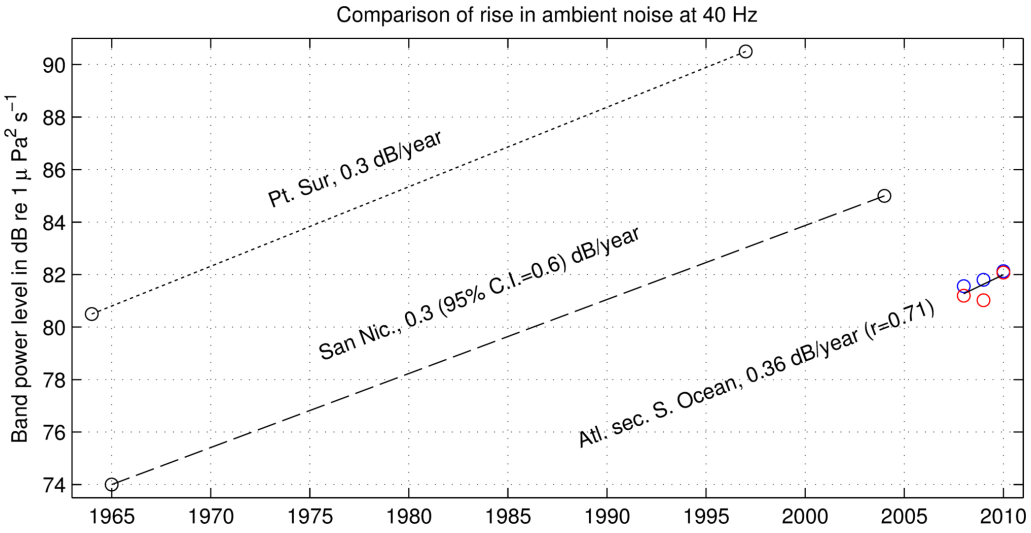

Figure 30: Comparison of yearly mean ambient noise SPL_{RMS} at 40 Hz, derived from McDonald et al. (2006), Andrew et al. (2002) and Wenz (1962). Circles display yearly averages, red represents Aural 69°S and blue Aural 66°S. Pt. Sur stands for measurements in the Pacific, from the cabled hydrophone array off Point Sur in California. San Nic. stands for measurements in the Pacific, with a cabled hydrophone array and autonomous recorders off San Nicholas Island in California. Atl. sec. S, Ocean stands for results from this thesis, derived from autonomous recorders in the Atlantic sector of the Southern Ocean.

Looking at the development of ambient noise as described by McDonald et al. (2006),Andrew et al. (2002) and Frisk (2012) an evaluation of the long term development of ambient noise is needed. They used band power levels averaged over different years in a 40 Hz band to detect an increase in ambient noise. The exact boundaries of the observed band were not given in the papers. To compare the SPL measurements of this thesis with their data, I calculated the yearly mean (only over those sections of the year that were covered each year) at 40 Hz (bandwidth was 0.5 Hz). A regression through these values results in a rise of 0.36 dB per year (r = 0.71) at 40 Hz. The development of 40 Hz ambient noise derived from previous measurement and this thesis is shown in Figure 30. It has to be stated that 3 years of measurements are not enough to securely detect a long term trend. But the measured trend of 0.36 db re 1 μPa^2 s^{-1} per year at 40 Hz fits well to the 0.3 dB per year trends reported by McDonald et al. (2006), Andrew et al. (2002) and Frisk

(2012). Increasing global marine traffic may result in rising low frequency noise levels, even in the remote polar oceans. Alternatively climate change and natural variation may lead to more or stronger storms.

The low frequency continuous noise indicators given by the EU Marine framework directive show the similar results. Figure 31 and 32 show the annual mean broadband and 63 Hz and 125 Hz third-octave band SPL. The yearly broadband SPL from Aural 66°S and Aural 69°S differs, no clear trend seems apparent. In the annually averaged broadband spectra, variation can especially be seen between 100 - 400 Hz, the frequency range of the Bioduck sound. In the annually averaged broadband spectra from Aural 69°S in Figure 32, differences between the years can be seen between 150 - 10000 Hz. This is the wind influenced part of the ambient noise spectrum, a difference in wind speed and sea ice distribution might have caused the observed difference.

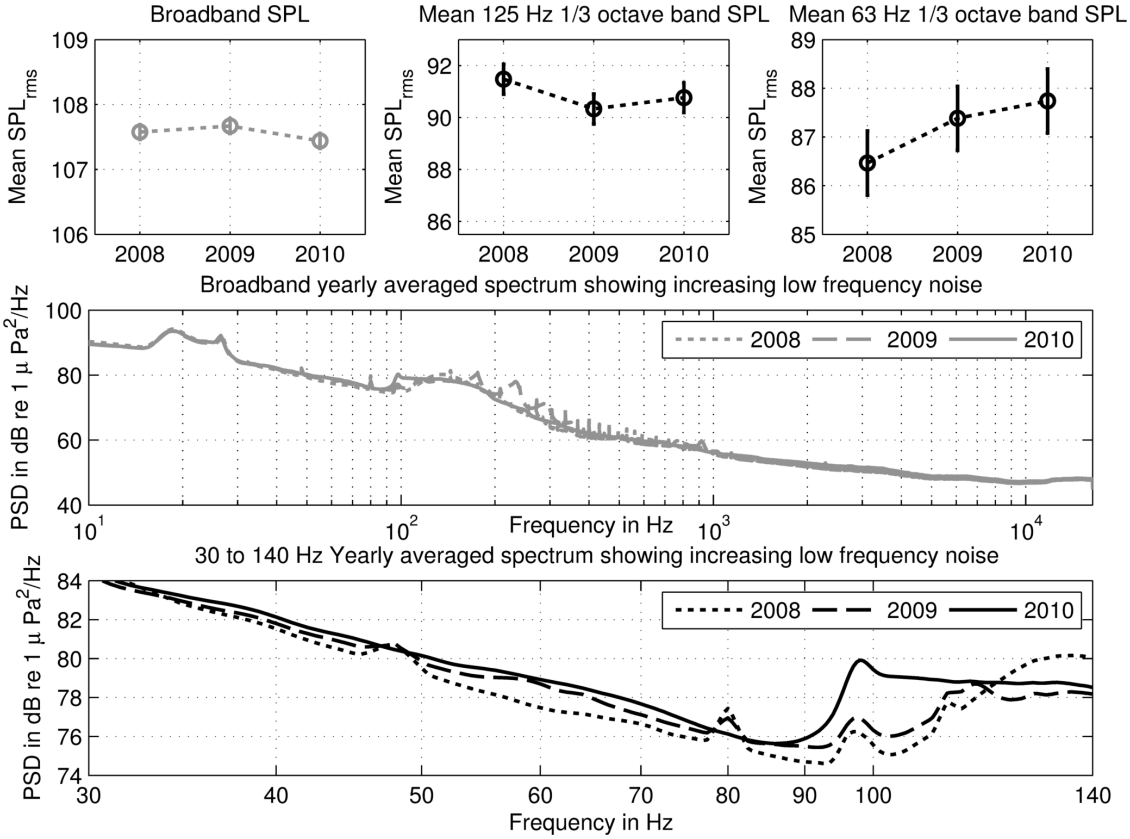

Figure 31: Yearly averaged broadband and 63 Hz and 125 Hz third-octave band and spectra of ambient noise from Aural 66°S. Upper plot show yearly mean SPL_{RMS} values, left side: broadband SPL_{RMS}, middle: 125 Hz third-octave band SPL_{RMS}, right side: 63 Hz third-octave band SPL_{RMS}. Middle spectrum shows mean broadband spectra for each recorded year. Lower plot shows low frequency spectrum from 30 - 140 Hz for each recorded year. Only recordings from those sections of the year that were covered each year were averaged

As seen in the topmost middle plot of Figure 31 and 32, the yearly averaged 125 Hz third-octave band SPL over the recorded years shows the same pattern for both Aurals. A view into the yearly averaged low frequency spectrum (lower spectrum) reveals a different spectral composition of the Bioduck chorus each year. Therewith it influences ambient noise in the 125 Hz third-octave band.

In contradiction to the broadband and 125 third-octave bands, the 63 Hz third-octave band shows a clear trend in yearly averaged SPL. The frequency band is not influenced by marine mammal noise bands and displays purely physically created noise. A regression of the yearly averaged SPL from both Aurals gives a rise of 0.65 db re 1 μPa per year (r = 0.77). This is a stronger trend than in the 40 Hz band. This can be seen in the yearly averaged low frequency spectra as well, the distance between the spectra at 40 Hz is less than at 63 Hz. Despite the intense inter annual noise dynamics an increase in low frequency ambient noise can be detected.

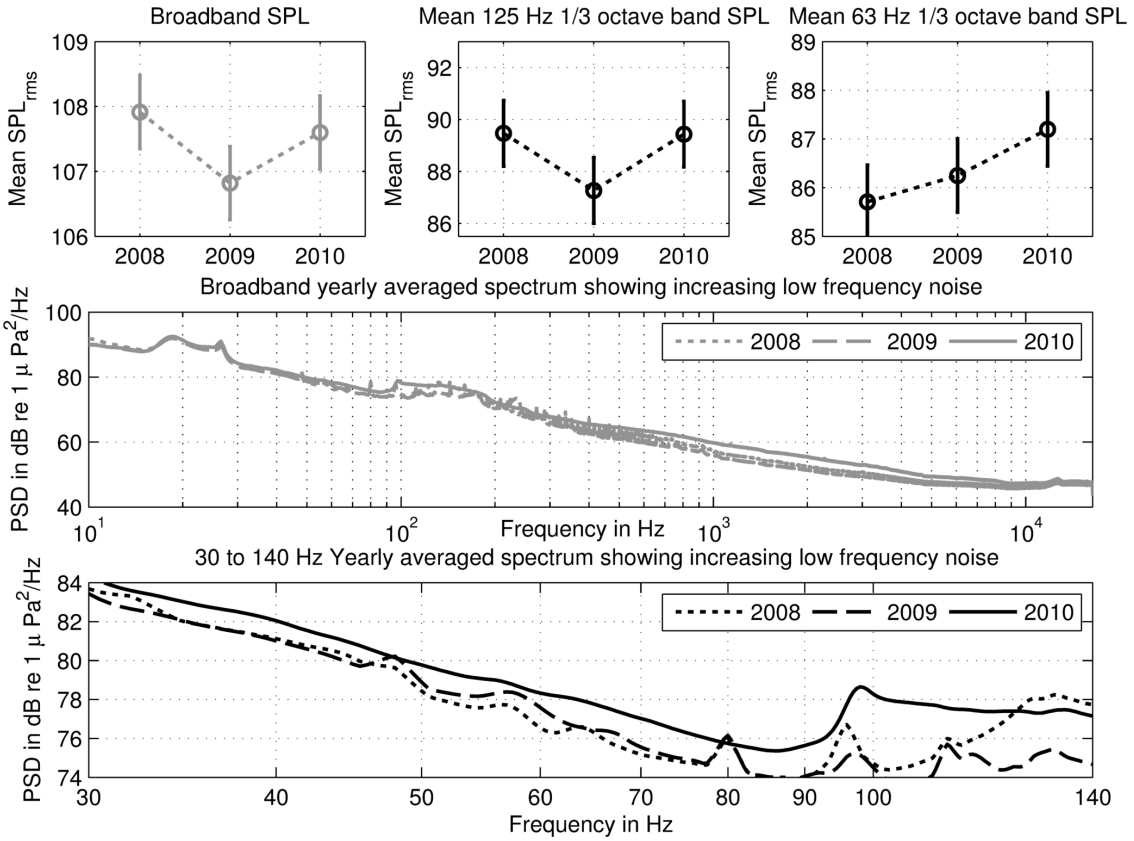

Figure 32: Yearly averaged broadband and 63 Hz and 125 Hz third-octave band and spectra of ambient noise from Aural 69°S. Upper plot show yearly mean SPL_{RMS} values, left side: broadband SPL_{RMS}, middle: 125 Hz third-octave band SPL_{RMS}, right side: 63 Hz third-octave band SPL_{RMS}. Middle spectrum shows mean broadband spectra for each recorded year. Lower plot shows low frequency spectrum from 30 - 140 Hz for each recorded year. Only recordings from those sections of the year that were covered each year were averaged

6.3. Recommendations for noise regulation

Taking into account the broad variation of ambient noise in time and frequency, regulation of ambient noise in the Southern Ocean needs careful planning. Of the two continuous low frequency noise indicators used in this thesis (SPL third-octave bands), one is influenced by unidentified vocalisations. The 125 Hz third-octave band lies in the frequency range of the Bioduck chorus, in Antarctic winter this chorus is the main contributor to ambient noise in this band. The 63 Hz third-octave band is unaffected by marine mammal induced noise. Ambient noise in this frequency band is only influenced by wind, waves and the ice cover. Since the occurrence, source and distribution of the Bioduck calls is largely unknown I would recommend not to use the 125 Hz third-octave band to monitor anthropogenic ambient noise. But it is quite suitable to study the development of the Bioduck chorus.

To avoid interference with marine mammal choruses the best frequency to monitor low frequency continuous noise in the Southern Ocean are between 30 - 90 Hz. However, it is crucial to consider the dynamics of the ambient noise when analysing noise levels. The data and analysis presented in this study can be used as baseline for further research and monitoring of ambient noise in the Atlantic sector of the Southern Ocean.

7. Conclusions

Wind, waves, ice and marine mammals influence the ambient noise prevailing in the Atlantic sector of the Southern Ocean (see overview plot in Figure 15). The annual dynamic is driven by seasonal changes in the ice cover. A yearly increase of 0.36 db re 1 μPa$^2 s^{-1}$ at 40 Hz has been detected. This agrees with findings of McDonald et al. (2006). Considering the EU marine framework good environmental status descriptors concerning low frequency continuous noise, noise in the 63 Hz third-octave band rises 0.65 db re 1 μPa per year.

If the low frequency noise continues to rise linear with time, noise levels will double in about 16 years. The implications this could have for marine life in the Southern Ocean, should be investigated. In addition to shipping noise, decreasing sea ice coverage could result in a noise increase. So far the Antarctic sea ice extent is not decreasing (Cavalieri and Parkinson, 2008). But due to ongoing global warming, the future of Antarctic sea ice remains uncertain. A reduced sea ice cover would not quieten ambient noise in Antarctic winter, so winter noise levels could rise 4.25 dB db re 1 μPa. If climate change leads to an increase in storms, ambient noise levels rise as well. Melting ice covers result in nosier oceans, whether this poses a threat to acoustically active animals remains to be investigated.

The observed ambient noise was highly dynamic in time and frequency. Variation occurs on multiple scales and reveals information about the process causing the noise. By listening to the continuous ambient noise, is possible to conclude about noise generating processes on the sea surface, including information on ice and wind. Several species of marine mammals have a signature in the noise, thus it is possible to determine the acoustic presence of blue, fin and possibly minke whales from the ambient noise. The decrease of blue whale vocalisations frequency has been confirmed. A previously unknown circadian pattern in the Bioduck chorus (possibly minke whales) occurs in the beginning of Antarctic winter and might be connected to feeding behaviour. Thus marine mammal noise bands not only carry information about the presence of animals, but also about seasonally distinct behaviour. Also leopard and crabeater seal presence can be detected in the ambient noise. It has been demonstrated that long term passive acoustic monitoring of the Southern Oceans ambient noise, provides information on biological, physical and possibly anthropogenic activities.

8. Outlook

While investigating ambient noise in the Southern Ocean many new questions arose. Future studies need to investigate the origin and purpose of Bioduck calls as well as the function of most known vocalisations. The findings of this thesis shall be published in a paper, to provide baseline information to scientists and policy makers. Future monitoring and noise regulations can use the results as reference.

During RV Polarstern cruise ANT-29-2 further recorders will be recovered and new ones deployed. The recordings from these recorders will be analysed for ambient noise and transient sounds. Also the multi year acoustic data set from the PALAOA acoustic observatory on the coast of Dronning-Maud land, can be analysed using the methods of this study. In the next month, it is planned to rewrite the Matlab™ code of this thesis and create an easy to use Matlab™ function or software. It will be distributed as open source code. The ambient noise dynamics of the Southern Ocean need to be monitored, so changes due to anthropogenic activity, from shipping to climate change, can be detected. Still, after all studies and investigations, sound in the oceans remains a fascinating and mysterious subject.

9. References

Acoustical Society of America (1986). American National Standard - Specification for Octave-Band and Fractional-Octave-Band Analog and Digital Filters.

Andrew, R. K., Howe, B. M., Mercer, J. a., and Dzieciuch, M. a. (2002). Ocean ambient sound: Comparing the 1960s with the 1990s for a receiver off the California coast. *Acoustics Research Letters Online*, 3(2):65.

Arveson, P. T. and Vendittis, D. J. (2000). Radiated noise characteristics of a modern cargo ship. *The Journal of the Acoustical Society of America*, 107(1):118–129.

Au, W. W. L. and Hastings, M. C. (2008). *Principles of Marine Bioacoustics*. Springer US, New York, NY.

Blickley, J. and Patricelli, G. (2010). Impacts of Anthropogenic Noise on Wildlife: Research Priorities for the Development of Standards and Mitigation. *Journal of International Wildlife Law & Policy*, 13(4):274–292.

Boyd, I. (2008). The effects of anthropogenic sound A draft research strategy. Technical Report June.

Branch, T. A., Matsuoka, K., and Miyashita, T. (2004). Evidence for Increases in Antarctic Blue whales based on Bayesian Modelling. *Marine Mammal Science*, 20(4):726–754.

Cavalieri, D. J. and Parkinson, C. L. (2008). Antarctic sea ice variability and trends, 1979 – 2006. *Journal of Geophysical Research*, 113(C7):1–19.

Clark, C., Ellison, W., Southall, B., Hatch, L., Van Parijs, S., Frankel, a., and Ponirakis, D. (2009). Acoustic masking in marine ecosystems: intuitions, analysis, and implication. *Marine Ecology Progress Series*, 395:201–222.

Clark, C. W. and Gagnon, G. C. (2006). Considering the temporal and spatial scales of noise exposures from seismic surveys on baleen whales. *Int. Whal. Comm.*, SC/58/E9.

Commission, E. (2010). Commission Decision of 1 September 2010 on criteria and methodological standards on good environmental status of marine waters. *Official Journal of the European Union*, 232(2008):14–24.

Committee on Potential Impacts of Ambient Noise in the Ocean on Marine Mammals, N. R. C. (2003). *Ocean Noise and Marine Mammals*. The National Academies Press.

Di Iorio, L. and Clark, C. W. (2010). Exposure to seismic survey alters blue whale acoustic communication. *Biology letters*, 6(1):51–4.

Flores, H., van Franeker, J. A., Siegel, V., Haraldsson, M., Strass, V., Meesters, E. H., Bathmann, U., and Wolff, W. J. (2012). The association of Antarctic krill Euphausia superba with the under-ice habitat. *PloS one*, 7(2):e31775.

Frisk, G. V. (2012). Noiseonomics: the relationship between ambient noise levels in the sea and global economic trends. *Scientific reports*, 2(1):437.

Gaten, E., Tarling, G., Dowse, H., Kyriacou, C., and Rosato, E. (2008). Is vertical migration in Antarctic krill (Euphausia superba) influenced by an underlying circadian rhythm? *Journal of genetics*, 87(5):473–83.

Gavrilov, A. N., McCauley, R. D., and Gedamke, J. (2012). Steady inter and intra-annual decrease in the vocalization frequency of Antarctic blue whales. *The Journal of the Acoustical Society of America*, 131(6):4476–4480.

Gedamke, J., Costa, D. P., Dunstan, A., Xplorer, U. N. E., Box, P. O., and Douglas, P. (2001). Localization and visual verification of a complex minke whale vocalization a). 109(6):3038–3047.

Halpern, B. S., Walbridge, S., Selkoe, K. A., Kappel, C. V., Micheli, F., D'Agrosa, C., Bruno, J. F., Casey, K. S., Ebert, C., Fox, H. E., Fujita, R., Heinemann, D., Lenihan, H. S., Madin, E. M. P., Perry, M. T., Selig, E. R., Spalding, M., Steneck, R., and Watson, R. (2008). A global map of human impact on marine ecosystems. *Science (New York, N.Y.)*, 319(5865):948–52.

Hildebrand, J. (2009). Anthropogenic and natural sources of ambient noise in the ocean. *Marine Ecology Progress Series*, 395:5–20.

Ichii, T. and Kato, H. (1991). Food and daily food consumption of southern minke whales in the Antarctic. *Polar Biology*, 11(7):479–487.

Kastak, D., Southall, B. L., Schusterman, R. J., and Kastak, C. R. (2005). Underwater temporary threshold shift in pinnipeds: Effects of noise level and duration. *The Journal of the Acoustical Society of America*, 118(5):3154.

Kibblewhite, a. C. and Jones, D. a. (1976). Ambient noise under Antarctic sea ice. *The Journal of the Acoustical Society of America*, 59(4):790.

Klinck, H., Mellinger, D. K., Klinck, K., Hager, J., Kindermann, L., and Boebel, O. (2010). Long-range underwater vocalizations of the crabeater seal (Lobodon carcinophaga). *The Journal of the Acoustical Society of America*, 128(1):474–9.

Knudsen, V. ., Alford, R. S., and Emling, J. W. (1948). Underwater Ambient Noise. *J. Mar. Res.*, 7:410.

Lurton, X. (2002). *An Introduction to Underwater Acoustics: Principles and Applications*. Springer Praxis Books. Springer.

Ma, B. B., Nystuen, J. A., and Lien, R.-c. (2005). Prediction of underwater sound levels from rain and wind. *The Journal of the Acoustical Society of America*, 117(6):3555.

Madsen, P. T. (2005). Marine mammals and noise: Problems with root mean square sound pressure levels for transients. *The Journal of the Acoustical Society of America*, 117(6):3952.

Matthews, D., Macleod, R., Mccauley, R. D., Division, M. O., Stirling, H., Maritime, W. A., and Division, O. (2004). Bio-Duck Activity in the Perth Canyon . An Automatic Detection Algorithm . Experimental data Auto-Detection Algorithm. (November):63–66.

McCauley, R. D., Fewtrell, J., Duncan, A. J., Jenner, C., Jenner, M. N., Penrose, J. D., Prince, R. I. T., Adhitya, A., Murdoch, J., and Mccabe, K. (2000). Marine seismic surveys - A study of environmental implications. *APPEA Journal*, 40:692–708.

McDonald, M., Hildebrand, J., and Mesnick, S. (2009). Worldwide decline in tonal frequencies of blue whale songs. *Endangered Species Research*, 9(December):13–21.

Mcdonald, M. A. (2006). Biogeographic characterisation of blue whale song worldwide: using song to identify populations. *Journal of cetacean research management*, 8(1):55 – 65.

McDonald, M. A., Calambokidis, J., Teranishi, A. M., and Hildebrand, J. a. (2001). The acoustic calls of blue whales off California with gender data. *The Journal of the Acoustical Society of America*, 109(4):1728.

McDonald, M. A., Hildebrand, J. A., and Wiggins, S. M. (2006). Increases in deep ocean ambient noise in the Northeast Pacific west of San Nicolas Island, California. *The Journal of the Acoustical Society of America*, 120(2):711.

Mckenna, M. F., Ross, D., Wiggins, S. M., and Hildebrand, J. A. (2012). Underwater radiated noise from modern commercial ships. 131(1).

Medwin, H. (2005). *Sounds in the Sea: From Ocean Acoustics to Acoustical Oceanography*. Cambridge University Press.

Medwin, H. and Clay, C. S. (1998). *Fundamentals of Acoustical Oceanography*. Academic Press.

Mellinger, K., Carson, D., and Clark, W. (2000). Characteristics of minke whale (Balaenoptera Acutorostrata) pulse trains recorded near Puerto Rico. *Marine Mammal Science*, 16(4):739–756.

Merchant, N. D., Blondel, P., Dakin, D. T., and Dorocicz, J. (2012). Averaging underwater noise levels for environmental assessment of shipping. 132(October):343–349.

Milne, a. R. (1972). Thermal Tension Cracking in Sea Ice: A Source of Underice Noise. *Journal of Geophysical Research*, 77(12):2177–2192.

Moore, S. E., Stafford, K. M., Melling, H., Berchok, C., Wiig, O. y., Kovacs, K. M., Lydersen, C., and Richter-Menge, J. (2011). Comparing marine mammal acoustic habitats in Atlantic and Pacific sectors of the High Arctic: year-long records from Fram Strait and the Chukchi Plateau. *Polar Biology*, 35(3):475–480.

Nichols, R. H. (1981). Infrasonic ambient ocean noise measurements: Eleuthera. *The Journal of the Acoustical Society of America*, 69(4):974–981.

Nieukirk, S. L., Mellinger, D. K., Moore, S. E., Klinck, K., Dziak, R. P., and Goslin, J. (2012). Sounds from airguns and fin whales recorded in the mid-Atlantic Ocean, 1999-2009. *The Journal of the Acoustical Society of America*, 131(2):1102–12.

Ospar (2009). Assessment of the environmental impact of underwater noise 2009. *Commission Report*, Biodiversi:1–44.

Perrin, W. F., Würsig, B. G., and Thewissen, J. G. M. (2009). *Encyclopedia of Marine Mammals*. Academic.

Pritchard, R. S. (1990). Sea ice noise-generating processes. *The Journal of the Acoustical Society of America*, 88(6):2830–2842.

Rogers, T. L., Cato, D. H., and Bryden, M. M. (1996). Behavioural significance of underwater vocalisations of captive Leopard Seals, Hydurga Leptonyx. *Marine Mammal Science*, 12(3):414–427.

SCAR (2012). Anthropogenic Sound in the Southern Ocean : an Update. In *Antarctic Treaty Consultative Meeting XXXV*, pages 1–11.

Schlitzer, R. (2012). Ocean Data View.

Scott, K. N. (2004). International Regulation of Undersea Noise. *International and Comparative Law Quarterly*, 53(April):287–324.

Sirović, A., Hildebrand, J. A., and Wiggins, S. M. (2007). Blue and fin whale call source levels and propagation range in the Southern Ocean. *The Journal of the Acoustical Society of America*, 122(2):1208–15.

Smith, S. W. (2003). *Digital Signal Processing: A Practical Guide for Engineers and Scientists*. Demystifying Technology Series. Newnes.

Spreen, G., Kaleschke, L., and Heygster, G. (2008). Sea ice remote sensing using AMSR-E 89-GHz channels. *Journal of Geophysical Research*, 113(C2).

Teschke, M., Wendt, S., Kawaguchi, S., Kramer, A., and Meyer, B. (2011). A circadian clock in Antarctic krill: an endogenous timing system governs metabolic output rhythms in the euphausid species Euphausia superba. *PloS one*, 6(10):e26090.

Thiele, D., Chester, E. T., and Gill, P. C. (2000). Cetacean distribution off Eastern Antarctica (80–150E) during the Austral summer of 1995/1996. *Deep Sea Research Part II: Topical Studies in Oceanography*, 47(12-13):2543–2572.

Tyack, P. L. (2008). Implications for marine mammals of large-scale changes in the marine acoustic environment. *Journal of Mammalogy*, 89(3):549–558.

Urick, R. J. (1983). *Principles of underwater sound*. McGraw-Hill.

Uscinski, B. J. and Wadhams, P. (1999). Ice-ocean acoustic energy transfer : ambient noise in the ice-edge region. *Deep Sea Research Part II: Topical Studies in Oceanography*, 46:1319–1333.

Van Opzeeland, I., Van Parijs, S., Bornemann, H., Frickenhaus, S., Kindermann, L., Klinck, H., Plötz, J., and Boebel, O. (2010). Acoustic ecology of Antarctic pinnipeds. *Marine Ecology Progress Series*, 414:267–291.

Širović, A., Hildebrand, J. a., Wiggins, S. M., McDonald, M. a., Moore, S. E., and Thiele, D. (2004). Seasonality of blue and fin whale calls and the influence of sea ice in the Western Antarctic Peninsula. *Deep Sea Research Part II: Topical Studies in Oceanography*, 51(17-19):2327–2344.

Weilgart, L. S. (2007). A Brief Review of Known Effects of Noise on Marine Mammals. *International Journal of Comparative Psychology*, 20(2):159–168.

Wenz, G. M. (1962). Acoustic Ambient Noise in the Ocean : Spectra and Sources. *The Journal of the Acoustical Society of America*, 34(12):1936–1956.

A. Abbreviations

SPL	Sound pressure level
PSD	Power spectral density
IWC	International whaling commission
RV	Research vessel
CTD	Conductivity, temperature and depth
RMS	Root mean square
GT	Gross Tonnage
GDP	Gross domestic product
PAM	Passive acoustic monitoring
RAM	Random access memory
TCXO	Temperature compensated crystal oscillator
FFT	Fast Fourier transform
ECMWF	European Centre for Medium-Range Weather Forecasts
AMSR-E	Advanced Microwave Scanning Radiometer for Earth Observation System

B. List of Figures

C. Technical Information

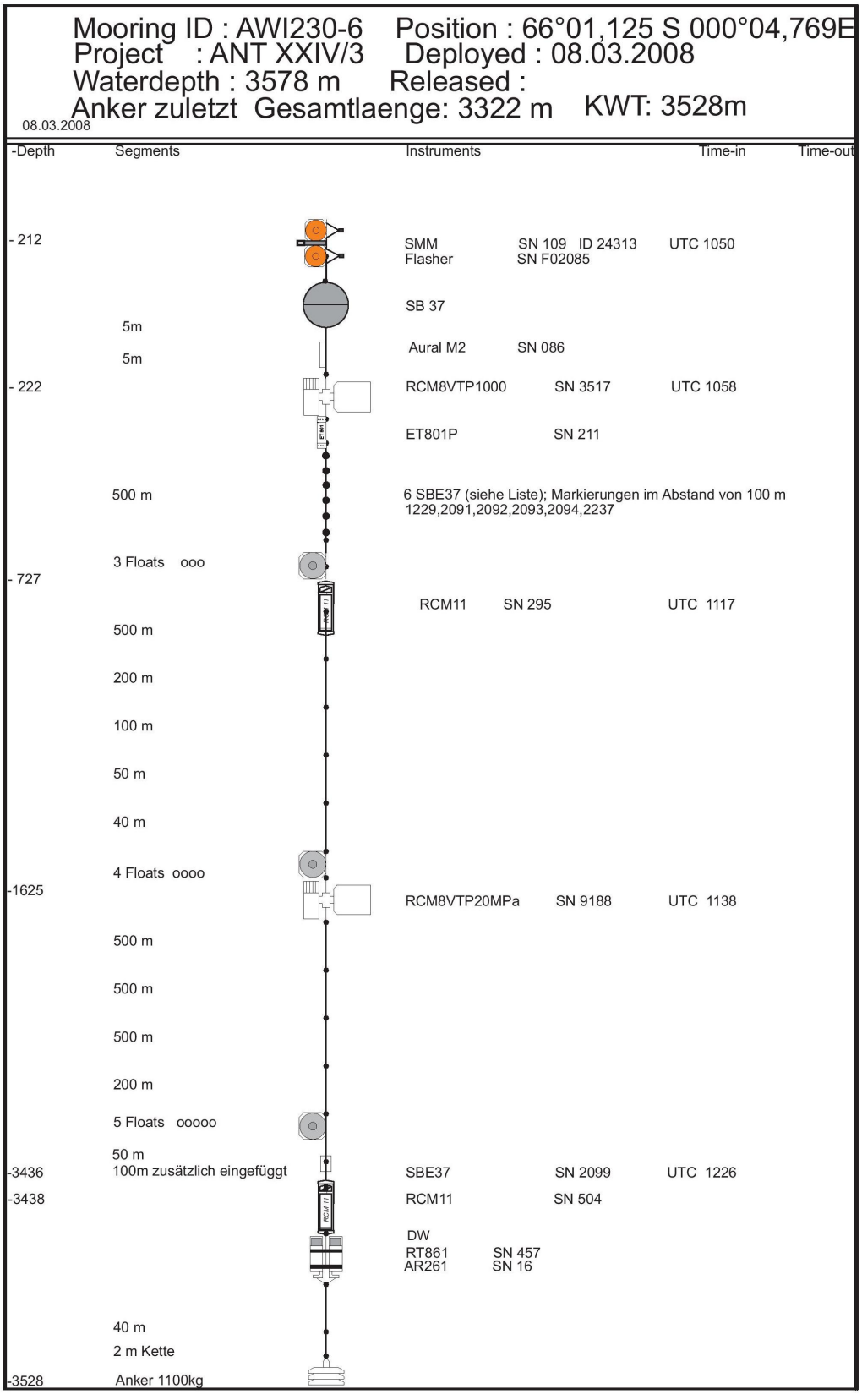

Figure 33: Technical drawing of Mooring AWI 230-6, by Mathias Monees and Olaf Strothman

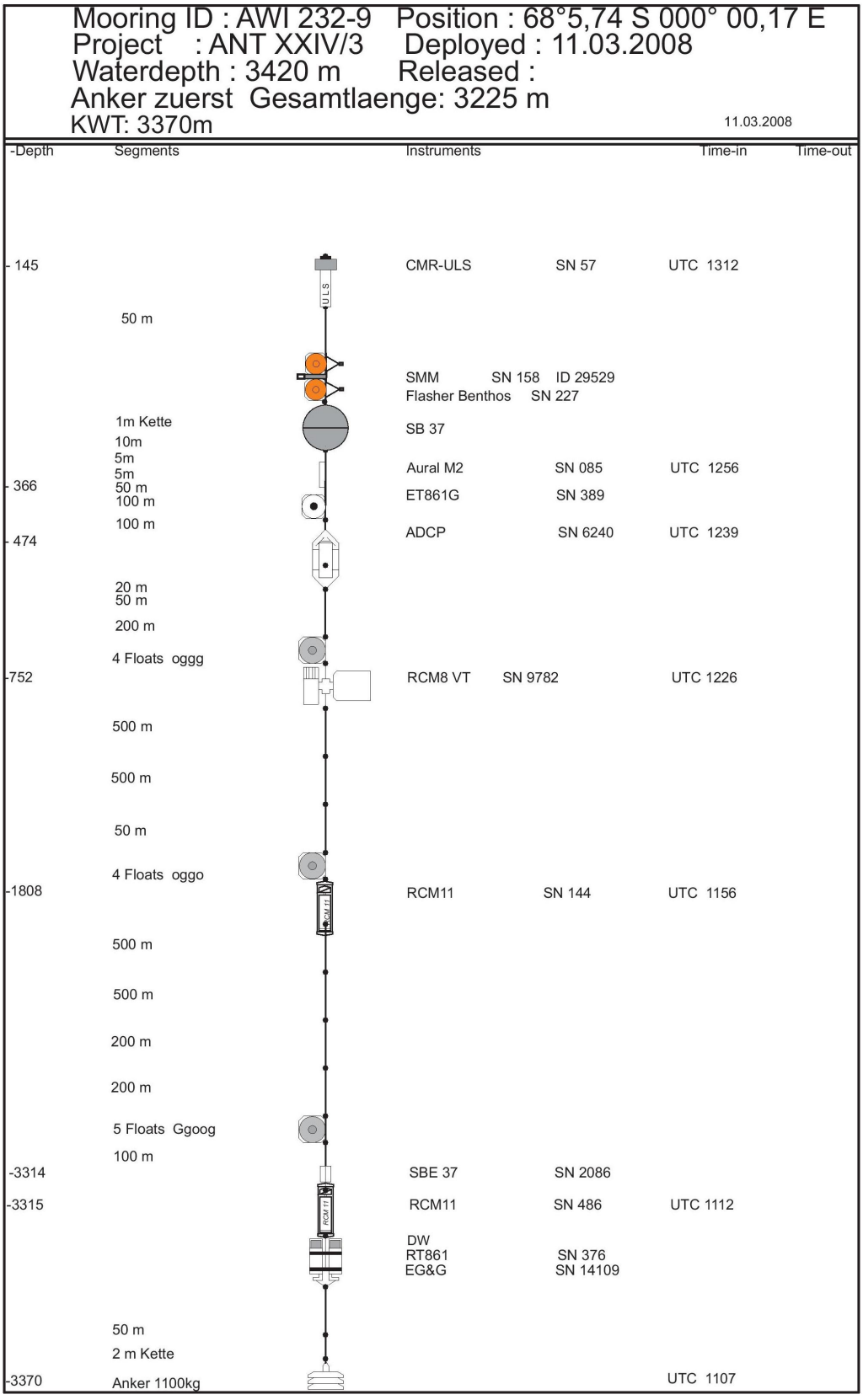

Figure 34: Technical drawing of Mooring AWI 232-9, by Mathias Monees and Olaf Strothman

Specifications subjects to change without notice

AURAL-M2
Specification Sheet

General

Supply Voltage: 12Vdc nominal (9Vdc to 15Vdc)
Operating temperature: 0 °C to 40 °C
Tested depth: 300 meters
Case Material: Stainless Steel 316, Delrin, Fiberglass Epoxy
Anode Material: Zinc

Power requirement	AURAL-M2 Release 2, 3 & 4
Standby	~ 8mA
Active - Wait to Record mode "5 sec"	~ 47 mA
Active - Record mode	~ 58mA
Active - Saving mode	~ 253mA

Analog Section

A/D: 16 bits
Filter: Programmable frequency 8th order linear phase low pass (Anti Aliasing)
Amplifier: Low Noise amplification with 16, 18, 20 & 22 dB selectable gain
Pressure Sensor: 0 to 1000 psi (0~682 m.) (resolution:1,3 cm, display: 0,1 m, accuracy: +/- 0,25 % max)
Temperature sensor: -10 °C to 40 °C (resolution: 0,0625 °C, display: 0,1 m, accuracy: +/- 0,5 °C)
Hydrophone: HTI-96-MIN
Usable Frequency range: 10 to 128, 256, 512, 1024, 2048, 4096, 8192, 16 384 Hz

Digital Section

MCU: 33 MIPS Dallas DS89C450 Ultra High Speed Flash Microcontroller
Flash Type & Size: Compact Flash 1 GB or more
Hard Disk Size: 2.5 inches Hard disk 320 GB or more
Hard Disk Data Transfer Speed: 1.5 MB/Sec
Time Base: Low Power 32.768 KHz TCXO with +/- 2ppm accuracy
Communication: RS232 (38.4Kbs, N, 8, 1)
System File Format: FAT32
Audio File Format: WAV
Sampling Rate: 256, 512, 1024, 2048, 4096, 8192, 16 384, 32 768 samples/second

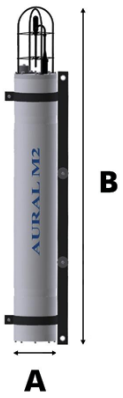

Units Information	16 batteries	64 batteries	128 batteries
A Diameter (1)	14,6 cm (5,75 in)	14,6 cm (5,75 in)	14,6 cm (5,75 in)
B Lenght	90 cm (35,375 in)	120 cm (47,375 in)	178 cm (70 in)
In air weight (2) (5)	20 Kg (45 lb)	32 Kg (71,5 lb)	49 Kg (109 lb)
In water weight (2) (4) (5)	9 Kg (19,5 lb)	14 Kg (30,5 lb)	21 Kg (46 lb)
Battery capacity (3)	30 Ah	120 Ah	240 Ah
Shipping case	-	16 Kg / 19 Kg 35,27 lb / 41,89 lb	21 Kg (46,30 lb)

(1) Cylinder only (without strap) (3) Battery capacity using Energizer EN95 (Based on 15mA constant drain)
(2) Including EN95 Batteries (4) Submerged in fresh water (5) Valid informations for AURALs made since 01-01-09

MULTI ÉLECTRONIQUE
1, 8e Avenue - Rimouski (Québec) G5L 2L9 - Canada Tel: 418 724-5835 - Fax: 418 722-4837
info@multi-electronique.com www.multi-electronique.com

Figure 35: Specifications sheet of the AURAL-M2 underwater recorder from Multi-Electronique (MTE) Inc.

D. Selected Matlab™ code

Listing 1: Find quietest 10 s and calculate power spectral density values after Welch from .wav files

```
% the ultimate 3 year spectrogram script by sebastian menze
%

%% Constants

dBFS=149; %db re 1uPa re v_full_scale
criticalsize=19000000; %in bytes

load( Data—AURAL2.mat ) %includes Aural data from Lars Kinderman, AWI

%% create data structure array for aural2

%create filename and pathname array
D.pathname= E:\RECORDER\aural2 ;
if ¬isfield(D, filename ) D.filename=dir(fullfile(D.pathname, *.wav )); end
D.index=1:size(D.filename,1);


%% new loop

for i=1:size(D.filename,1)

    tic
    disp([ File number:   num2str(i)]);

      D.starttime(i)=Data.Content(1,i).starttime;



     %check if there is distorted files, leave them out
     if D.filename(i,1).bytes<criticalsize
          warning( bad file, swicth to next one );

          calcmean(i)=1;

         continue
     else
        calcmean(i)=0;



     try

```

```
44      filename=D.filename(i,1).name; %creates variable for filename(for
            wavread function)
45      [wav,FS]=wavread([D.pathname  \  char(filename)]); %stores normalized
            signal data under filename
46      D.FS=FS; %saves FS — Frequency sampling
47      signal=power(10,(dBFS/20))*wav; %convert data.signal to uPa
48
49
50            % search the quietest second
51            signalsize=size(signal,1);
52       second10=FS*10;%lenght of one second
53       t=300/signalsize; %smallest time distance in s
54
55       %convolute data with second long rectangular filter (average over 1 s)
56       signalpositive=signal.^2;
57
58       cs=cumsum(signalpositive);
59       dcs=cs(second10+1:end)-cs(1:end-second10);
60
61       [~,ixmin]=min(dcs);
62       quietsec=signal(ixmin:ixmin+second10-1);
63
64       [~,ixmax]=max(dcs);
65       loudsec=signal(ixmax:ixmax+second10-1);
66
67
68       % spectrum
69
70      samplerate=FS;
71      FFTsize=2^16;
72
73
74      [D.spec_quiet_10s(:,i),Fp]=pwelch(quietsec,[],[],FFTsize,samplerate);
75      D.spec_quiet_10s(:,i)=10*log10(D.spec_quiet_10s(:,i));
76
77
78      [D.spec_5min(:,i),Fp]=pwelch(signal,[],[],FFTsize,samplerate);
79      D.spec_5min(:,i)=10*log10(D.spec_5min(:,i));
80
81        [D.spec_loud_10s(:,i),Fp]=pwelch(loudsec,[],[],FFTsize,samplerate);
82      D.spec_loud_10s(:,i)=10*log10(D.spec_loud_10s(:,i));
83
84       D.frequency=Fp   ;
85
86      catch  err
87      warning( it did not work :-( );
88      pause(60)
89      return
90      end
91
92
93      toc
94
95       end
96
97
98            if i>2 & calcmean(i-1)==1;
99
```

```
100             D.spec_quiet_10s(:,i-1)=(D.spec_quiet_10s(:,i-2)+D.spec_quiet_10s
                    (:,i))/2;
101             D.spec_5min(:,i-1)=(D.spec_5min(:,i-2)+D.spec_5min(:,i))/2;
102             D.spec_loud_10s(:,i-1)=(D.spec_loud_10s(:,i-2)+D.spec_loud_10s(:,
                    i))/2;
103           end
104
105
106 end
107
108
109
110 save( D_aural2 , D , -v7.3 )
111
112
113 clear
114
115 %%%%%%%%%%%%%%%%%%%%%%%%%%%%%%%%%%%%%%%%%%%%%%%%%%%%%%%%%%%%%%%%%%%%%%%%%%%%
116
117 %% create data structure array for aural1
118 load( Data-AURAL1.mat ) %includes Aural data from Lars Kinderman, AWI
119
120 %create filename and pathname array
121 D.pathname= \\Csysp235\g\RECORDER\DATA\aural1 ;
122 if ~isfield(D, filename ) D.filename=dir(fullfile(D.pathname, *.wav )); end
123 D.index=1:size(D.filename,1);
124
125
126 %% new loop
127
128 for i=1:size(D.filename,1)
129
130     tic
131     disp([ File number:   num2str(i)]);
132
133       D.starttime(i)=Data.Content(1,i).starttime;
134
135
136
137      %check if there is distorted files, leave them out
138      if D.filename(i,1).bytes<criticalsize
139           warning( bad file, swicth to next one );
140
141           calcmean(i)=1;
142
143          continue
144      else
145         calcmean(i)=0;
146
147
148
149      try
150
151     filename=D.filename(i,1).name; %creates variable for filename(for
            wavread function)
152     [wav,FS]=wavread([D.pathname  \  char(filename)]); %stores normalized
            signal data under filename
153     D.FS=FS; %saves FS - Frequency sampling
```

```
154       signal=power(10,(dBFS/20))*wav; %convert data.signal to uPa
155
156
157            % search the quietest second
158            signalsize=size(signal,1);
159        second10=FS*10;%lenght of one second
160        t=300/signalsize; %smallest time distance in s
161
162        %convolute data with second long rectangular filter (average over 1 s)
163        signalpositive=signal.^2;
164
165        cs=cumsum(signalpositive);
166        dcs=cs(second10+1:end)-cs(1:end-second10);
167
168        [~,ixmin]=min(dcs);
169        quietsec=signal(ixmin:ixmin+second10-1);
170
171        [~,ixmax]=max(dcs);
172        loudsec=signal(ixmax:ixmax+second10-1);
173
174
175        % spectrum
176
177       samplerate=FS;
178       FFTsize=2^16;
179
180
181       [D.spec_quiet_10s(:,i),Fp]=pwelch(quietsec,[],[],FFTsize,samplerate);
182       D.spec_quiet_10s(:,i)=10*log10(D.spec_quiet_10s(:,i));
183
184
185       [D.spec_5min(:,i),Fp]=pwelch(signal,[],[],FFTsize,samplerate);
186       D.spec_5min(:,i)=10*log10(D.spec_5min(:,i));
187
188         [D.spec_loud_10s(:,i),Fp]=pwelch(loudsec,[],[],FFTsize,samplerate);
189       D.spec_loud_10s(:,i)=10*log10(D.spec_loud_10s(:,i));
190
191        D.Frequency=Fp;
192
193       catch  err
194       warning( it did not work :-( );
195       pause(60)
196       return
197       end
198
199
200       toc
201
202        end
203
204
205            if i>2 & calcmean(i-1)==1;
206
207            D.spec_quiet_10s(:,i-1)=(D.spec_quiet_10s(:,i-2)+D.spec_quiet_10s
                   (:,i))/2;
208            D.spec_5min(:,i-1)=(D.spec_5min(:,i-2)+D.spec_5min(:,i))/2;
209            D.spec_loud_10s(:,i-1)=(D.spec_loud_10s(:,i-2)+D.spec_loud_10s(:,
                   i))/2;
```

```
210           end
211
212
213 end
214
215 save( D_aural1 , D , -v7.3 )
```

Listing 2: Read ECMWF grid and extract variables

```
1  %% read ECMWF Weather Data from DAT files to matlab variables
2
3  pathname= E:\ECMWF-Wetterdaten\TEMP\ ;
4  w.filename=dir(fullfile(pathname, *.DAT ));
5
6  %% create grid information
7
8  griddif=1.125;
9  w.lat=linspace(-49.500,-79.875,28);
10
11 for i=1:104
12     grid_lon_var = 70.875-(griddif*(i-1));
13     w.lon(i) = -grid_lon_var;
14 end
15 %% find position in grid
16
17 D1.lon=0.0028;
18 D1.lat=-68.9957;
19
20 lookuplat=D1.lat;
21 lookuplon=D1.lon;
22
23 [~,i_lat]=min(abs(lookuplat-w.lat));
24 [~,i_lon]=min(abs(lookuplon-w.lon));
25
26 %% process each year
27
28 for counter1=1:size(w.filename,1)
29
30 temp_raw=dlmread([pathname w.filename(counter1,1).name],  );
31
32 % read time
33 w.time=[];
34 for i=1:29:size(temp_raw,1)
35  w.time=[ w.time temp_raw(i,1) ];
36 end
37
38 switch counter1
39     case 1
40     w.time= datenum(2008,1,1,0,0,0)+w.time;
41     case 2
42     w.time= datenum(2009,1,1,0,0,0)+w.time;
43     case 3
44     w.time= datenum(2010,1,1,0,0,0)+w.time;
45 end
46
47 %read temp
48    index=[];
```

```
49      for ii=2:29:size(temp_raw,1)
50          index=[index ii];
51   temp(:,:,ii)=temp_raw(ii:ii+27,:) ;
52      end
53
54  for iii=1:size(w.time,2)
55    w.temp(:,:,iii)=temp(:,:,index(iii));
56  end
57
58  for i=1:size(w.time,2)
59   w.position(i)=w.temp(i_lat,i_lon,i);
60  end
61
62  expr=[ w  num2str(counter1)  =w; ];
63  evalin( base ,expr);
64
65  clear temp_raw w.temp w.time w.position
66  end
67
68  w.time=[w1.time w2.time w3.time];
69  datestr(w.time(1))
70  datestr(w.time(end))
71  w.temp_position=[w1.position w2.position w3.position];
```

Listing 3: Read sea ice concentration from sea ice data grid

```
1  % variables
2
3  D1.lon=0.0028;
4  D1.lat=-68.9957;
5
6  D2.lat=-66.01875;
7  D2.lon=00.079483333333333;
8
9  % read latlon_grid ./ICE_raw/h5/LongitudeLatitudeGrid-s6250-Antarctic.h5
10 filename_grid =  C:\Users\smenze\Documents\MATLAB\seaice\
       LongitudeLatitudeGrid-s6250-Antarctic.hdf ;
11
12 lon = hdfread(filename_grid,  Longitudes );
13 lat = hdfread(filename_grid,  Latitudes );
14
15 [diflatx,i_diflat]=min(abs(D1.lon-lon(:))+abs(D1.lat-lat(:)));
16
17 lat(i_diflat)
18 lon(i_diflat)
19
20 for years=2008:2010
21
22 icecon.pathname=[ C:\Users\smenze\Documents\MATLAB\seaice\  num2str(years)
       \ ]
23
24 %create filename and pathname array
25 %icecon.pathname= C:\Users\smenze\Documents\MATLAB\seaice\2008;
26 icecon.filename=dir(fullfile(icecon.pathname, *.nc ));
27 icecon.index=1:size(icecon.filename,1);
28
29
```

```
for i=1:size(icecon.filename,1)

len(years-2007)=size(icecon.filename,1) ;

ncid = netcdf.open([icecon.pathname icecon.filename(i).name],  NOWRITE );

% ncdisp([icecon.pathname  \  icecon.filename(i).name]) % gibt dir info
    ber das file aus

ice = netcdf.getVar(ncid, 2); % valid range ist 0-1; missing values = -999

netcdf.close(ncid);

icecon.ice(years-2007,i)=ice(i_diflat);
icecon.time(years-2007,i)=datenum(str2num(icecon.filename(i).name(11:14)),
    ...
                                  str2num(icecon.filename(i).name(15:16)),
                                      ...
                                  str2num(icecon.filename(i).name(17:18)));

disp([ sea ice conc at   datestr(icecon.time(years-2007,i))  is   num2str(
    icecon.ice(i))   percent! ])

clear ice

end

end

icecon.ice=[icecon.ice(1,1:len(1)) icecon.ice(2,1:len(2)) icecon.ice(3,1:
    len(3))];
icecon.time=[icecon.time(1,1:len(1)) icecon.time(2,1:len(2)) icecon.time
    (3,1:len(3))];


h=figure(1)
area(icecon.time,icecon.ice)
datetick( x , mm-yyyy , keeplimits )
```

Listing 4: Correlate power spectral density time series with wind speed time series under different ice conditions

```
%% ice dependend
noiceindex=D1.icecon==0;

x=D1.windspeed(noiceindex);

for i=1:size(D1.Frequency,1)
y=D1.spec_quiet_10s(i,noiceindex);

C=cov(x,y);
p1(i)=C(2)/(std(x)*std(y));

disp(num2str(i));
end

semilogx(p1)
```

```
xlim([10 D1.FS]); grid on

%%

fulliceindex=find(D1.icecon==1);

x=D1.windspeed(fulliceindex);

for i=1:size(D1.Frequency,1)
y=D1.spec_quiet_10s(i,fulliceindex);

C=cov(x,y);
p2(i)=C(2)/(std(x)*std(y));

disp(num2str(i));
end

semilogx(p2)
xlim([10 D1.FS]); grid on

%%

figure(2)
set(gcf, color ,[1 1 1]);

subplot(2,1,1)
semilogx(linspace(0,D1.FS/2,size(p1,2)),p1, -g )
xlim([10 D1.FS/2]); grid on
ylim([-0.05 0.6]);
title( 0% ice cover );
xlabel( Frequency in Hz );
ylabel( Correlation coefficient );

subplot(2,1,2)
semilogx(linspace(0,D1.FS/2,size(p2,2)),p2, -g )
xlim([10 D1.FS/2]); grid on
ylim([-0.05 0.6]);
title( 100% ice cover )
xlabel( Frequency in Hz );
ylabel( Correlation coefficient );

hold on

% export_fig spectrum_correlation_windspeed_ice.png -r200

%% ice dependend
noiceindex=D2.icecon==0;

x=D2.windspeed(noiceindex);

for i=1:size(D2.Frequency,1)
y=D2.spec_quiet_10s(i,noiceindex);

C=cov(x,y);
p1(i)=C(2)/(std(x)*std(y));

disp(num2str(i));
end
```

```
74
75  semilogx(p1)
76  xlim([10 D2.FS]); grid on
77
78  %%
79
80  fulliceindex=find(D2.icecon==1);
81
82  x=D2.windspeed(fulliceindex);
83
84  for i=1:size(D2.Frequency,1)
85  y=D2.spec_quiet_10s(i,fulliceindex);
86
87  C=cov(x,y);
88  p2(i)=C(2)/(std(x)*std(y));
89
90  disp(num2str(i));
91  end
92
93  semilogx(p2)
94  xlim([10 D2.FS]); grid on
95
96  %%
97
98  figure(2)
99  set(gcf, color ,[1 1 1]);
100
101 subplot(2,1,1)
102 semilogx(linspace(0,D2.FS/2,size(p1,2)),p1, -b )
103 xlim([10 D2.FS/2]); grid on
104 ylim([-0.05 0.6]);
105 title( 0% ice cover );
106 xlabel( Frequency in Hz );
107 ylabel( Correlation coefficient );
108
109 subplot(2,1,2)
110 semilogx(linspace(0,D2.FS/2,size(p2,2)),p2, -b )
111 xlim([10 D2.FS/2]); grid on
112 ylim([-0.05 0.6]);
113 title( 100% ice cover )
114 xlabel( Frequency in Hz );
115 ylabel( Correlation coefficient );
116
117 % export_fig spectrum_correlation_windspeed_ice.png -r200
```

Listing 5: Create Wenz like overview plot of ambient noise

```
1  % wenz style plot (southern ocean)
2
3  figure(1)
4  set(gcf, Color ,[1 1 1], Renderer ,  painter );
5  clf
6  windowsize=5;
7  fullscale=149;
8  SPL_scale = 0:0.25:fullscale;
9  n_points=size(D66.rms_broad_quiet,2)
10
```

```
[counts_per_bin,bin] = histc(D66.rms_broad_quiet,SPL_scale);
cumulative_cpb = cumsum(counts_per_bin);
cumulative_cpb=cumulative_cpb/n_points;

%% ice cdf
% quiet
x=0.05;
ix_x=cumulative_cpb>x;
louderthan01=min(SPL_scale(ix_x));

%loud
x=0.95;
ix_x=cumulative_cpb>x;
louderthan90=min(SPL_scale(ix_x));

%mean
x=0.50;
ix_x=cumulative_cpb>x;
louderthan=min(SPL_scale(ix_x));


frequencyborders=[10,16000];
frequencyborders_index= D66.Frequency==frequencyborders(1,1) ;
index=1:D66.FS;
ilow=index(frequencyborders_index==1)
frequencyborders_index= D66.Frequency==frequencyborders(1,2) ;
ihigh=index(frequencyborders_index==1)


semilogx(D66.Frequency,filtfilt(ones(1,windowsize)/windowsize,1,mean(
    D66.spec_quiet_10s(:,D66.rms_broad_quiet>louderthan & D66.icecon==1),2))
    , color ,[0.5 0.5 0.5], linewidth ,2)
 xlim([10 16000])
  ylim([40 105])
  grid on
hold all



xxx=[D66.Frequency(ilow:ihigh) ;  flipud(D66.Frequency(ilow:ihigh)) ];
yyy=[filtfilt(ones(1,windowsize)/windowsize,1,mean(D66.spec_quiet_10s(ilow:
    ihigh,D66.rms_broad_quiet>louderthan01 & D66.icecon==1),2)) ;  flipud(
    filtfilt(ones(1,windowsize)/windowsize,1,mean(D66.spec_quiet_10s(ilow:
    ihigh,D66.rms_broad_quiet>louderthan90 & D66.icecon==1),2)))];
ccc=[0.7 0.7 0.7];
fillhandle=patch(xxx,yyy,ccc);
set(fillhandle, Facecolor ,ccc, EdgeColor , none );
icecdf=fillhandle
%% noice cdf

% quiet
x=0.05;
ix_x=cumulative_cpb>x;
louderthan01=min(SPL_scale(ix_x));

%loud
x=0.95;
ix_x=cumulative_cpb>x;
```

```
louderthan90=min(SPL_scale(ix_x));


frequencyborders=[10,16000];
frequencyborders_index= D66.Frequency==frequencyborders(1,1) ;
index=1:D66.FS;
ilow=index(frequencyborders_index==1)
frequencyborders_index= D66.Frequency==frequencyborders(1,2) ;
ihigh=index(frequencyborders_index==1)

% semilogx(D66.Frequency,filtfilt(ones(1,windowsize)/windowsize,1,mean(
    D66.spec_quiet_10s(:,D66.rms_broad_quiet>louderthan & D66.icecon==0),2))
    , color ,[0 0 0], linewidth ,2)
%  xlim([10 16000])
%   ylim([40 105])
%   grid on
% hold on
%


xxx=[D66.Frequency(ilow:ihigh) ;  flipud(D66.Frequency(ilow:ihigh)) ];
yyy=[filtfilt(ones(1,windowsize)/windowsize,1,mean(D66.spec_quiet_10s(ilow:
    ihigh,D66.rms_broad_quiet>louderthan01 & D66.icecon==0),2)) ;  flipud(
    filtfilt(ones(1,windowsize)/windowsize,1,mean(D66.spec_quiet_10s(ilow:
    ihigh,D66.rms_broad_quiet>louderthan90 & D66.icecon==0),2)))];
ccc=[0.5 0.5 0.5];
fillhandle=patch(xxx,yyy,ccc);
set(fillhandle, Facecolor ,ccc, EdgeColor , none );
noicecdf=fillhandle


%% wind values no ice

windowsize=100;



frequencyborders=[10,16000];
frequencyborders_index= D66.Frequency==frequencyborders(1,1) ;
index=1:D66.FS;
ilow=index(frequencyborders_index==1)
frequencyborders_index= D66.Frequency==frequencyborders(1,2) ;
ihigh=index(frequencyborders_index==1)

windnoice=semilogx(D66.Frequency(ilow:ihigh),filtfilt(ones(1,windowsize)/
    windowsize,1,mean(D66.spec_quiet_10s(ilow:ihigh,D66.windspeed>0 &
    D66.windspeed<9 & D66.icecon==0),2)), color ,[0 0 0], linestyle , - ,
    linewidth ,2)
semilogx(D66.Frequency(ilow:ihigh),filtfilt(ones(1,windowsize)/windowsize
    ,1,mean(D66.spec_quiet_10s(ilow:ihigh,D66.windspeed>9 & D66.windspeed<18
     & D66.icecon==0),2)), color ,[0 0 0], linestyle , - , linewidth ,2)
semilogx(D66.Frequency(ilow:ihigh),filtfilt(ones(1,windowsize)/windowsize
    ,1,mean(D66.spec_quiet_10s(ilow:ihigh,D66.windspeed>18 & D66.windspeed
    <27 & D66.icecon==0),2)), color ,[0 0 0], linestyle , - , linewidth ,2)
xlim([10 16000])
  ylim([40 105])
  grid on
hold on
```

```
110
111 %% wind values ice
112
113 windowsize=100;
114
115
116
117 frequencyborders=[10,16000];
118 frequencyborders_index= D66.Frequency==frequencyborders(1,1) ;
119 index=1:D66.FS;
120 ilow=index(frequencyborders_index==1)
121 frequencyborders_index= D66.Frequency==frequencyborders(1,2) ;
122 ihigh=index(frequencyborders_index==1)
123
124 windice=semilogx(D66.Frequency(ilow:ihigh),filtfilt(ones(1,windowsize)/
        windowsize,1,mean(D66.spec_quiet_10s(ilow:ihigh,D66.windspeed>0 &
        D66.windspeed<9 & D66.icecon==1),2)), color ,[0 0 0], linestyle , '--' ,
        linewidth ,2)
125 semilogx(D66.Frequency(ilow:ihigh),filtfilt(ones(1,windowsize)/windowsize
        ,1,mean(D66.spec_quiet_10s(ilow:ihigh,D66.windspeed>9 & D66.windspeed<18
         & D66.icecon==1),2)), color ,[0 0 0], linestyle , '--' , linewidth ,2)
126 semilogx(D66.Frequency(ilow:ihigh),filtfilt(ones(1,windowsize)/windowsize
        ,1,mean(D66.spec_quiet_10s(ilow:ihigh,D66.windspeed>18 & D66.windspeed
        <27 & D66.icecon==1),2)), color ,[0 0 0], linestyle , '--' , linewidth ,2)
127 xlim([10 16000])
128   ylim([40 105])
129   grid on
130 hold on
131
132
133 %% blue whale
134 windowsize=1;
135
136 frequencyborders=[15,30];
137 frequencyborders_index= D66.Frequency==frequencyborders(1,1) ;
138 index=1:D66.FS;
139 ilow=index(frequencyborders_index==1)
140 frequencyborders_index= D66.Frequency==frequencyborders(1,2) ;
141 ihigh=index(frequencyborders_index==1)
142
143 x=0.50;
144 ix_x=cumulative_cpb>x;
145 louderthan=min(SPL_scale(ix_x));
146
147  x=0.05;
148  ix_x=cumulative_cpb>x;
149  louderthan01=min(SPL_scale(ix_x));
150
151 x=0.95;
152 ix_x=cumulative_cpb>x;
153 louderthan99=min(SPL_scale(ix_x));
154
155 xxx=[D66.Frequency(ilow:ihigh) ;  flipud(D66.Frequency(ilow:ihigh)) ];
156 yyy=[filtfilt(ones(1,windowsize)/windowsize,1,mean(D66.spec_quiet_10s(ilow:
        ihigh,D66.rms_broad_quiet>louderthan01 & D66.icecon==1),2)) ;  flipud(
        filtfilt(ones(1,windowsize)/windowsize,1,mean(D66.spec_quiet_10s(ilow:
        ihigh,D66.rms_broad_quiet>louderthan99),2)))];
157 ccc=[0 0.5 1];
```

```
fillhandle=patch(xxx,yyy,ccc);
set(fillhandle, Facecolor ,ccc, EdgeColor , none );
bluecdf=fillhandle

hold on

bluemean=semilogx(D66.Frequency(ilow:ihigh),mean(D66.spec_quiet_10s(ilow:
    ihigh,D66.rms_broad_quiet>louderthan),2), color ,[0 0 1], linewidth ,2)
 xlim([10 16000])
  ylim([40 105])
  grid on
hold on
%

%% fin whale
windowsize=1;

frequencyborders=[93,105];
frequencyborders_index= D66.Frequency==frequencyborders(1,1) ;
index=1:D66.FS;
ilow=index(frequencyborders_index==1)
frequencyborders_index= D66.Frequency==frequencyborders(1,2) ;
ihigh=index(frequencyborders_index==1)

x=0.50;
ix_x=cumulative_cpb>x;
louderthan=min(SPL_scale(ix_x));

 x=0.05;
 ix_x=cumulative_cpb>x;
 louderthan01=min(SPL_scale(ix_x));

x=0.95;
ix_x=cumulative_cpb>x;
louderthan99=min(SPL_scale(ix_x));

xxx=[D66.Frequency(ilow:ihigh) ;  flipud(D66.Frequency(ilow:ihigh)) ];
yyy=[filtfilt(ones(1,windowsize)/windowsize,1,mean(D66.spec_quiet_10s(ilow:
    ihigh,D66.rms_broad_quiet>louderthan01 & D66.icecon==1),2)) ;  flipud(
    filtfilt(ones(1,windowsize)/windowsize,1,mean(D66.spec_quiet_10s(ilow:
    ihigh,D66.rms_broad_quiet>louderthan99 & D66.icecon==1),2)))];
ccc=[0 1 0.5];
fillhandle=patch(xxx,yyy,ccc);
set(fillhandle, Facecolor ,ccc, EdgeColor , none );
fincdf=fillhandle
hold on

finmean=semilogx(D66.Frequency(ilow:ihigh),filtfilt(ones(1,windowsize)/
    windowsize,1,mean(D66.spec_quiet_10s(ilow:ihigh,D66.rms_broad_quiet>
    louderthan ),2)), color ,[0 0.5 0], linewidth ,2)
 xlim([10 16000])
  ylim([40 105])
  grid on
hold on
%

%% bioduck
windowsize=5;
```

```
210
211 frequencyborders=[105,350];
212 frequencyborders_index= D66.Frequency==frequencyborders(1,1) ;
213 index=1:D66.FS;
214 ilow=index(frequencyborders_index==1)
215 frequencyborders_index= D66.Frequency==frequencyborders(1,2) ;
216 ihigh=index(frequencyborders_index==1)
217
218 x=0.50;
219 ix_x=cumulative_cpb>x;
220 louderthan=min(SPL_scale(ix_x));
221
222  x=0.05;
223  ix_x=cumulative_cpb>x;
224  louderthan01=min(SPL_scale(ix_x));
225
226 x=0.95;
227 ix_x=cumulative_cpb>x;
228 louderthan99=min(SPL_scale(ix_x));
229
230 xxx=[D66.Frequency(ilow:ihigh) ;  flipud(D66.Frequency(ilow:ihigh)) ];
231 yyy=[filtfilt(ones(1,windowsize)/windowsize,1,mean(D66.spec_quiet_10s(ilow:
        ihigh,D66.rms_broad_quiet>louderthan01 & D66.icecon==1),2)) ;  flipud(
        filtfilt(ones(1,windowsize)/windowsize,1,mean(D66.spec_quiet_10s(ilow:
        ihigh,D66.rms_broad_quiet>louderthan99 & D66.icecon==1),2)))];
232 ccc=[1 1 0];
233 fillhandle=patch(xxx,yyy,ccc);
234 set(fillhandle, Facecolor ,ccc, EdgeColor , none );
235 hold on
236 biocdf=fillhandle
237
238 biomean=semilogx(D66.Frequency(ilow:ihigh),filtfilt(ones(1,windowsize)/
        windowsize,1,mean(D66.spec_quiet_10s(ilow:ihigh,D66.rms_broad_quiet>
        louderthan & D66.icecon==1),2)), color ,[1 0.7 0], linewidth ,2)
239  xlim([10 16000])
240   ylim([40 105])
241   grid on
242 hold on
243 %
244
245 %% leopard seal
246 windowsize=10;
247
248 frequencyborders=[280,370];
249 frequencyborders_index= D66.Frequency==frequencyborders(1,1) ;
250 index=1:D66.FS;
251 ilow=index(frequencyborders_index==1)
252 frequencyborders_index= D66.Frequency==frequencyborders(1,2) ;
253 ihigh=index(frequencyborders_index==1)
254
255 timesta=datenum(2008,12,10);
256 timeend=datenum(2009,1,1);
257
258 x=0.50;
259 ix_x=cumulative_cpb>x;
260 louderthan=min(SPL_scale(ix_x));
261
262  x=0.05;
```

```
 ix_x=cumulative_cpb>x;
 louderthan01=min(SPL_scale(ix_x));

x=0.95;
ix_x=cumulative_cpb>x;
louderthan99=min(SPL_scale(ix_x));

xxx=[D66.Frequency(ilow:ihigh) ;  flipud(D66.Frequency(ilow:ihigh)) ];
yyy=[filtfilt(ones(1,windowsize)/windowsize,1,mean(D66.spec_quiet_10s(ilow:
    ihigh,D66.rms_broad_quiet>louderthan01 & D66.starttime>timesta &
    D66.starttime<timeend),2)) ;  flipud(filtfilt(ones(1,windowsize)/
    windowsize,1,mean(D66.spec_quiet_10s(ilow:ihigh,D66.rms_broad_quiet>
    louderthan99 & D66.starttime>timesta & D66.starttime<timeend),2)))];
ccc=[0.8 0 0.9];
fillhandle=patch(xxx,yyy,ccc);
set(fillhandle, Facecolor ,ccc, EdgeColor , none );
hold on
leocdf=fillhandle

leomean=semilogx(D66.Frequency(ilow:ihigh),filtfilt(ones(1,windowsize)/
    windowsize,1,mean(D66.spec_quiet_10s(ilow:ihigh,D66.rms_broad_quiet>
    louderthan & D66.starttime>timesta & D66.starttime<timeend),2)), color
    ,[0.5 0 0.5], linewidth ,2)
 xlim([10 16000])
  ylim([40 105])
  grid on
hold on
%

%% crabeater seal
windowsize=20;

frequencyborders=[401,1000];
frequencyborders_index= D66.Frequency==frequencyborders(1,1) ;
index=1:D66.FS;
ilow=index(frequencyborders_index==1)
frequencyborders_index= D66.Frequency==frequencyborders(1,2) ;
ihigh=index(frequencyborders_index==1)

timesta=datenum(2008,11,1);
timeend=datenum(2008,11,31);

fullscale=149;
SPL_scale = 0:0.25:fullscale;
n_points=size(D66.rms_broad_quiet(D66.starttime>timesta & D66.starttime<
    timeend),2)

[counts_per_bin,bin] = histc(D66.rms_broad_quiet(D66.starttime>timesta &
    D66.starttime<timeend),SPL_scale);
cumulative_cpb = cumsum(counts_per_bin);
cumulative_cpb=cumulative_cpb/n_points;

x=0.50;
ix_x=cumulative_cpb>x;
louderthan=min(SPL_scale(ix_x));

 x=0.05;
 ix_x=cumulative_cpb>x;
```

```
 louderthan01=min(SPL_scale(ix_x));

x=0.95;
ix_x=cumulative_cpb>x;
louderthan99=min(SPL_scale(ix_x));

xxx=[D66.Frequency(ilow:ihigh) ;  flipud(D66.Frequency(ilow:ihigh)) ];
yyy=[filtfilt(ones(1,windowsize)/windowsize,1,mean(D66.spec_quiet_10s(ilow:
    ihigh,D66.rms_broad_quiet>louderthan01 & D66.starttime>timesta &
    D66.starttime<timeend),2)) ;  flipud(filtfilt(ones(1,windowsize)/
    windowsize,1,mean(D66.spec_quiet_10s(ilow:ihigh,D66.rms_broad_quiet>
    louderthan99 & D66.starttime>timesta & D66.starttime<timeend),2)))];
ccc=[0 0.9 0.9];
fillhandle=patch(xxx,yyy,ccc);
set(fillhandle, Facecolor ,ccc, EdgeColor , none );

hold on
crabcdf=fillhandle

crabmean=semilogx(D66.Frequency(ilow:ihigh),filtfilt(ones(1,windowsize)/
    windowsize,1,mean(D66.spec_quiet_10s(ilow:ihigh,D66.rms_broad_quiet>
    louderthan & D66.starttime>timesta & D66.starttime<timeend),2)), color
    ,[0 0.5 0.8], linewidth ,2)
 xlim([10 16000])
  ylim([40 105])
  grid on
hold on
%

%% polarstern
% windowsize=20;
%
% semilogx(D66.Frequency,filtfilt(ones(1,windowsize)/windowsize,1,
    D66.spec_quiet_10s(:,1)), color ,[1 0 0], linewidth ,2)
%  xlim([10 16000])
%   ylim([40 105])
%   grid on
% hold on

%% title etc

title( \bf{Ocean ambient noise in the Atlantic sector of the Southern Ocean
    } , fontsize ,14)
ylabel( PSD in dB re 1 \mu Pa )
xlabel( Frequency in Hz )

ax1=gca;
ax2 = axes( position ,get(gca, position ), visible , off );


legend(ax1,[noicecdf, icecdf, windnoice, windice],...
 Open water surface conditions (5^t^h to 95^t^h percentile) , Ice covered
    surface conditions(5^t^h to 95^t^h percentile) ,...
 Open water wind speed dependency (0-9, 9-18, 18-27 m/s) , Ice cover wind
    speed dependency (0-9, 9-18, 18-27 m/s) )

legend(ax2,[fincdf,finmean,biocdf,biomean,leocdf,leomean,crabcdf,crabmean,
    bluecdf,bluemean],...
```

```
358  Fin whale chorus (5^t^h to 95^t^h percentile) , Median fin whale chorus ,
       ...
359  Bioduck chorus (5^t^h to 95^t^h percentile) , Median Bioduck chorus ,...
360  Leopard seal chorus (5^t^h to 95^t^h percentile) , Median Leopard seal
       chorus ,...
361  Crabeater seal chorus (5^t^h to 95^t^h percentile) , Median Crabeater seal
        chorus ,...
362  Blue whale Z-call chorus (5^t^h to 95^t^h percentile) , Median blue whale
       Z-call chorus )
363
364 % export_fig C:\Users\smenze\Dropbox\Bachelorthesis\figures\
       ambientnoise_southernocean.png -r300 -painters
```

E. Acknowledgements

I would like to thank my supervisors Oliver Zielinski and Olaf Boebel, who supported me with many ideas and suggestions. While preparing and writing this thesis I learned a lot from them: From programming with Matlab™ to scientific writing. For her help with the Aurals and much appreciated everyday support I thank Steffanie Rettig. Also Lars Kindermann greatly helped me with Matlab™ and answered many questions. I further want to thank Ilse van Opzeeland, Anette Bombosch, Elke Burkhardt and Daniel Zitterbart of the Ocean Acoustics working group. Thanks to Andreas Wisotzki for providing the CTD data and New Zealand based photographer John Weller for providing the cover picture. My parents greatly encouraged me during 3 years of studying and while writing this thesis, thanks for your support.

F. Declaration of Authorship

I hereby certify that the thesis I am submitting is entirely my own original work except where otherwise indicated.

Sebastian Menze